

Design and Synthesis of Poly ADP-ribose Polymerase-1 Inhibitors. 2. Biological Evaluation of Aza-5[*H*]-phenanthridin-6-ones as Potent, Aqueous-Soluble Compounds for the Treatment of Ischemic Injuries

Dana Ferraris,* Yao-Sen Ko, Thomas Pahutski, Rica Pargas Ficco, Larisa Serdyuk, Christina Alemu, Chadwick Bradford, Tiffany Chiou, Randall Hoover, Shirley Huang, Susan Lautar, Shi Liang, Qian Lin, May X.-C. Lu, Maria Mooney, Lisa Morgan, Yongzhen Qian, Scott Tran, Lawrence R. Williams, Qi Yi Wu, Jie Zhang, Yinong Zou, and Vincent Kalish

Guilford Pharmaceuticals Inc., 6611 Tributary Street, Baltimore, Maryland 21224

Received March 5, 2003

A series of aza-5[*H*]-phenanthridin-6-ones were synthesized and evaluated as inhibitors of poly ADP-ribose polymerase-1 (PARP-1). Inhibitory potency of the unsubstituted aza-5[*H*]-phenanthridin-6-ones (i.e., benzonaphthyridones) was dependent on the position of the nitrogen atom within the core structure. The A ring nitrogen analogues (7-, 8-, and 10-aza-5[*H*]-phenanthridin-6-ones) were an order of magnitude less potent than C ring nitrogen analogues (1-, 2-, 3-, and 4-aza-5[*H*]-phenanthridin-6-ones). Preliminary stroke results from 1- and 2-aza-5[*H*]-phenanthridin-6-one prompted structure–activity relationships to be established for several 2- and 3-substituted 1-aza-5[*H*]-phenanthridin-6-ones. The 2-substituted 1-aza-5[*H*]-phenanthridin-6-ones were designed to improve the solubility and pharmacokinetic profiles for this series of PARP-1 inhibitors. Most importantly, three compounds from this series demonstrated statistically significant protective effects in rat models of stroke and heart ischemia.

Introduction

Poly ADP-ribose polymerase-1 (PARP-1, EC 2.4.2.30) is an abundant nuclear enzyme with an important role in the cellular life cycle.^{1–3} The PARP-1 enzyme has three structural regions: the DNA binding domain containing two zinc fingers, the automodification domain, and the catalytic domain.^{4,5} The catalytic domain is responsible for converting nicotinamide adenine dinucleotide (NAD⁺) into nicotinamide and an ADP-ribose unit that is bound to the substrate protein or nucleotide segment.⁶ When overactivated, PARP-1 can cause the consumption of NAD⁺ and subsequently a drop in the level of intracellular ATP. This depletion of ATP results in cell death through a necrotic pathway and eventually in ischemic tissue damage.^{7,8} Many studies with PARP-1 “knockout” mice have established the protective effects against a stroke⁹ and a myocardial infarction (MI).¹⁰ More recently, studies have demonstrated the utility of PARP-1 inhibitors in rat models of stroke and MI,¹¹ indicating PARP-1 as a clinically relevant target for ischemic injuries.

Many of the early PARP-1 inhibitors are based on the structure of nicotinamide (Figure 1, structure A). For example, quinazolines¹² (Figure 1, structure B, X = N), isoquinolones¹³ (structure B, X = CH), and the closely related tricyclic 5[*H*]-phenanthridin-6-ones¹⁴ (structure C, R = H, Figure 1) are well-known classes of inhibitors whose structure–activity relationships have been established against PARP-1. It is generally accepted that the 5[*H*]-phenanthridin-6-one core competes with NAD⁺ (structure A, Figure 1, R = adenosine) for the nicotinamide binding pocket in the catalytic domain of PARP-

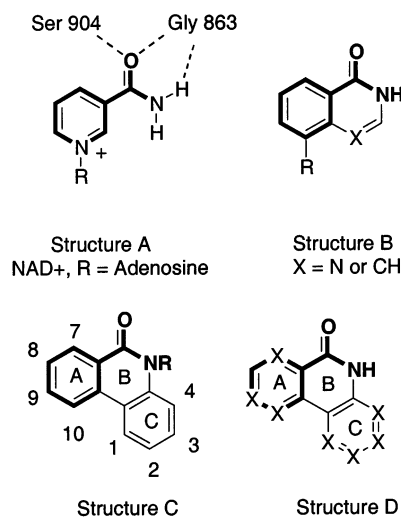
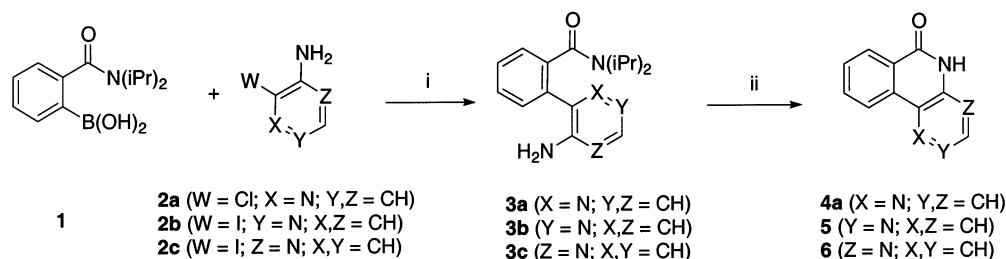


Figure 1. Structures of isoquinolones, 5[*H*]-phenanthridin-6-ones and related PARP-1 inhibitors.

1. Accordingly, the lone pairs of the 5[*H*]-phenanthridin-6-one oxygen bind to Ser904 and Gly863 while the amide nitrogen donates a hydrogen bond to Gly863.^{15,16} Any manipulation of this amide portion of the ring system results in decreased *in vitro* potency.¹⁷ There are few examples, however, of PARP-1 inhibitors with heteroatom replacements in the fused aryl rings of these inhibitors (highlighted in bold, Figure 1).¹⁸ In this manuscript, we present the aza-5[*H*]-phenanthridin-6-ones (structure D; one X is N, and all other X groups are CH) to better determine the *in vitro* and *in vivo* effects of heteroatom replacements within the 5[*H*]-phenanthridin-6-one core. We obtained information about the inhibitory effects of a ring-nitrogen atom on the nicotinamide binding pocket by testing the inhibi-

* To whom correspondence should be addressed. Phone: (410) 631-8126. Fax: (410) 631-6797. Email: ferrarisd@guilfordpharm.com.

Scheme 1^a

^a Reagents: (i) Pd(PPh₃)₄, K₂CO₃, toluene/EtOH (10:1), 73–85%; (ii) THF, 3 equiv of LDA, 78–94%.

tory potencies of 7-, 8-, and 10-aza-5[*H*]-phenanthridin-6-ones against PARP-1. In addition, the 1-, 2-, 3-, and 4-aza derivatives were tested to determine the in vitro and in vivo effects of a nitrogen atom in the C ring. Structure–activity relationship data, as well as preliminary rat stroke data, prompted us to derivatize this 1-aza-5[*H*]-phenanthridin-6-one core structure. Tertiary amines were incorporated into this core as solubilizing groups in an effort to administer these PARP-1 inhibitors as intravenous solutions, a necessity for acute clinical indications. Finally and most importantly, several examples of PARP-1 inhibitors from the 2-substituted 1-aza-5[*H*]-phenanthridin-6-one series demonstrate statistically significant efficacy in animal models of brain and heart ischemia (MCAO, MI) by intravenous administration.

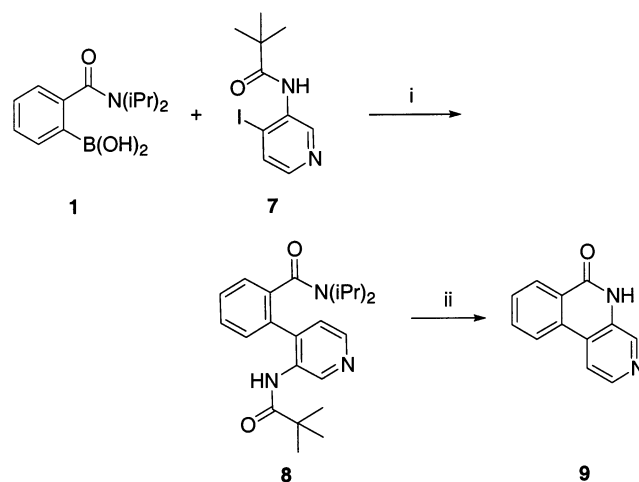
Results and Discussion

Chemistry. The synthesis of 1-, 2-, and 4-aza-5[*H*]-phenanthridin-6-ones **4a**, **5**, and **6** was carried out as outlined in Scheme 1. Commercially available 2-chloro-3-aminopyridine **2a** was coupled with boronic acid **1**¹⁹ under standard Suzuki conditions to yield biphenyl **3a** in 85% yield. Subsequent cyclization occurred in THF with the addition of 3 equiv of lithium diisopropylamide (LDA) to afford the parent 1-aza-5[*H*]-phenanthridin-6-one **4a** in 89% yield. The 2- and 4-aza derivatives **5**²⁰ and **6** were synthesized in a manner similar to that of **4a** using **2b** and **2c**, respectively.

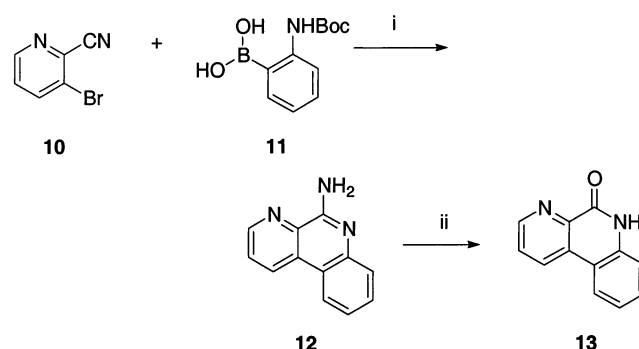
The synthesis of 3-aza-5[*H*]-phenanthridin-6-one **9** required amide **7**, which was synthesized according to the literature procedure in 23% overall yield from 3-aminopyridine (Scheme 2).²¹ Coupling of amide **7** with boronic acid **1** led to the amide **8** in 57% yield under Suzuki coupling conditions. The treatment of amide **8** with concentrated HCl afforded 3-aza-5[*H*]-phenanthridin-6-one **9** in 60% yield. This material was identical to the literature characterization of this compound.¹⁹

The 7-aza derivative was synthesized as indicated in Scheme 3. The boronic acid carbamate **11**²² was coupled with 2-cyano-3-bromopyridine **10** under standard Suzuki conditions leading directly to amine **12** in 29% yield. A diazotization of **12** was performed in H₂O/H₂SO₄ with NaNO₂ to afford the desired 7-aza-5[*H*]-phenanthridin-6-one **13** in 22% yield.

Synthesis of the 8- and 10-aza-derivatives **15a** and **15b** is outlined in Scheme 4. In one step, the coupling of boronic acid **11** and 4-chloronicotinic acid ethyl ester **14a** resulted in the cyclized 8-aza-5[*H*]-phenanthridin-6-one **15a** in one step in 24% yield. A similar cyclization and subsequent deprotection of the butoxycarbonyl

Scheme 2^a

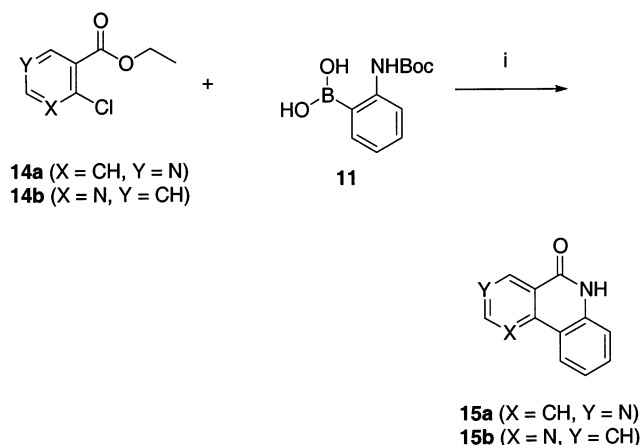
^a Reagents: (i) Pd(PPh₃)₄, 2.0 M Na₂CO₃, DME, 57%; (ii) concentrated HCl, 60%.

Scheme 3^a

^a Reagents: (i) Pd(PPh₃)₄, K₂CO₃, toluene/EtOH (10:1), 29%; (ii) H₂SO₄, NaNO₂, 0–100 °C, 22%.

group have been reported.²² This one-step coupling procedure was utilized with **14b**, affording **15b** in 19% yield.

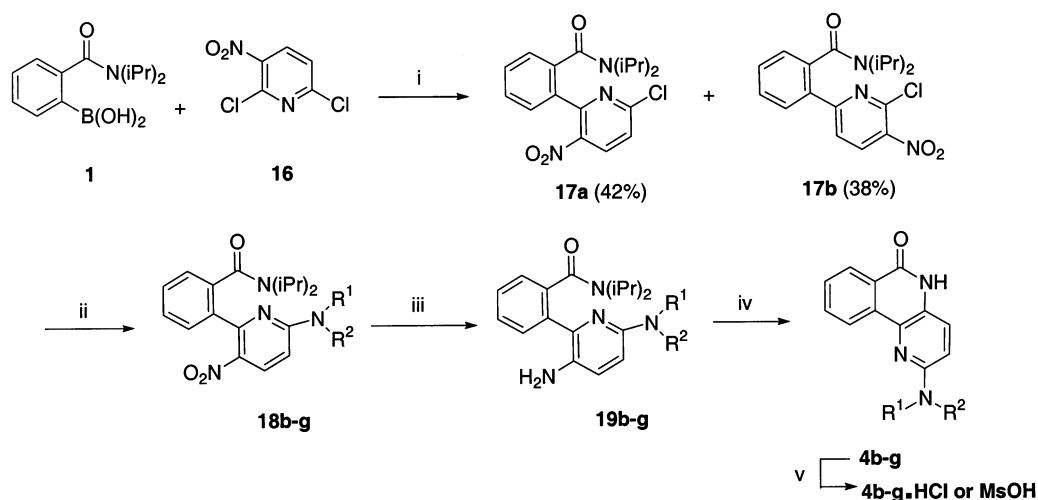
The 2-substituted 1-aza-5[*H*]-phenanthridin-6-ones were initially synthesized as illustrated in Scheme 5 (method A). Coupling of boronic acid **1** with commercially available 2,6-dichloro-3-nitropyridine **16** led to the nitro chloride **17a** in 42% yield. The moderate yield for this reaction can be explained by the isolation of the isomeric **17b** in approximately the same yield. Chromatographic separation of the two isomers was accomplished, and the desired isomer was aminated with various amines to yield nitroamines **18b–g** in yields ranging from 72% to 92%. The subsequent reduction of the nitro group under standard hydrogenation conditions led to the anilines **19b–g** in excellent yields.

Scheme 4^a

^a Reagents: (i) Pd(PPh₃)₄, K₂CO₃, toluene/EtOH (10:1), 19–24%.

The cyclization to 2-substituted 1-aza-5[*H*]-phenanthridin-6-ones was accomplished by using an excess of LDA (3 equiv) in tetrahydrofuran. This cyclization procedure afforded the desired compounds **4b–g** in moderate yields (42–46%). Salt formation was accomplished by suspending the requisite free base in tetrahydrofuran and addition of 1 equiv of acid (HCl in diethyl ether or methanesulfonic acid). The hydrochloride or mesylate salts (**4b–g**)·HCl or (**4b–g**)·MsOH precipitated out of solution and were collected by filtration. The inherent problems with method A occur with the LDA cyclization. These strongly basic conditions limit the number of functional groups that can be incorporated into the synthesis. This limitation in addition to the low yields led to the design of an alternative route (method B) outlined in Scheme 6.

To directly compare the two methods, compound **4g** was prepared by method B. The boronic ester **20** was prepared according to the literature²³ on a gram scale. The Suzuki coupling of **20** with 2,6-dichloro-3-nitropyridine **16** led to the desired isomer **21a** in 45% yield as well as 35% of the undesired species **21b**. Nucleophilic aromatic substitution of chloride **21a** was carried out using *N*-methylpiperazine, leading to the nitro ester **22a**. The improvement in the synthesis is accomplished

Scheme 5^a

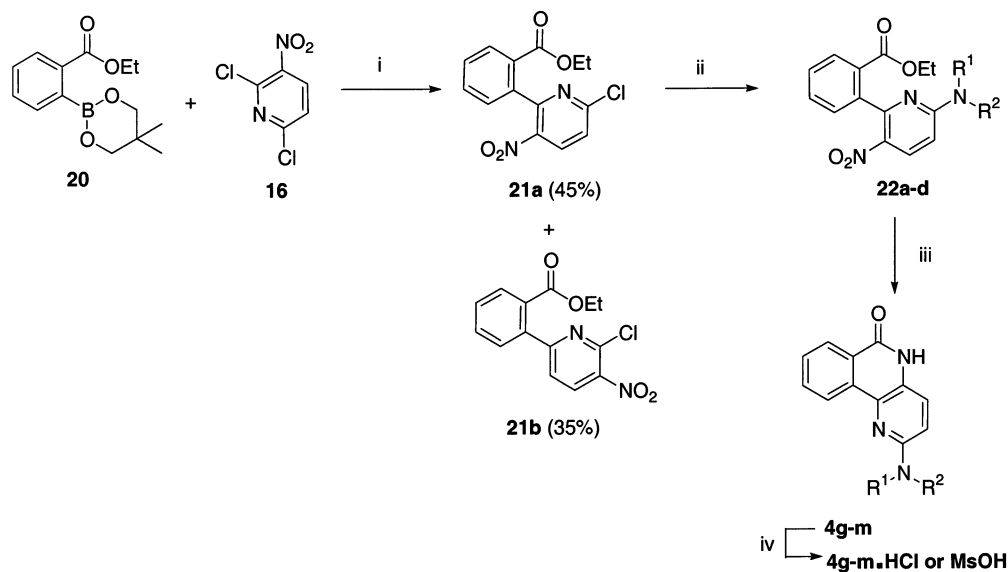
^a Method A. Reagents: (i) Pd(PPh₃)₄, K₂CO₃, toluene/EtOH (10:1); (ii) HNR₁R₂ (excess), DIEA, 72–92%; (iii) H₂/Pd/C, 90–100%; (iv) THF, 3 equiv of LDA, 42–46%; (v) 1 equiv of HCl or MsOH, 84–95%.

by a combination of the last two steps of Scheme 5 into one. Reduction of the nitro group with Raney nickel and hydrazine, followed by immediate cyclization of the amino ester, leads to 2-amino-1-aza-5[*H*]-phenanthridin-6-one **4g** in 29% overall yield compared to 14% overall yield using method A. Amines **4h–m** were also synthesized via method B using the requisite amines in overall yields of 20–30%. Salt formation was carried out as illustrated in Scheme 5 to form (**4g–m**)·HCl or (**4g–m**)·MsOH in 85–99% yield.

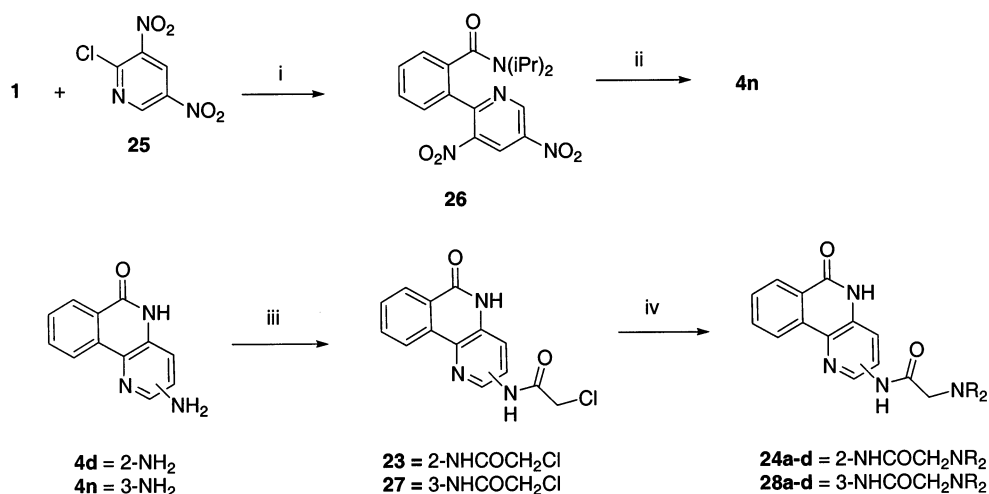
Further derivatization of amine **4d** was carried out as shown in Scheme 7. Acylation of **4d** with chloroacetyl chloride in dimethylacetamide led to the α -chloroamide **23** in 95% yield. Subsequent substitution of the activated chloride with various amines led to the subseries of amides **24a–e** in 82–92% yields.

Similarly, derivatization at the 3-position of 1-aza-5[*H*]-phenanthridin-6-ones was accomplished by first synthesizing 3-amino-1-aza-5[*H*]-phenanthridin-6-one **4n** from boronic acid **1** and 2-chloro-3,5-dinitropyridine **25** using standard Suzuki coupling conditions (see Scheme 7). Reduction of the intermediate dinitro ester **26** led to **4n**. Reduction of the nitro groups led to an intermediate diamine that cyclized to the desired 3-amino-1-aza-5[*H*]-phenanthridin-6-one **4n** in 55% overall yield from **26**. Acylation of this amine with chloroacetyl chloride led to the α -chloroamide **27** in 95% yield. Chloride **27** was aminated in a manner similar to that of the 2-substituted isomer **23** (Scheme 7) to afford amides **28a–d**.

Biological Evaluation and SAR Discussion. A comparative in vitro study of all aza-5[*H*]-phenanthridin-6-one derivatives with respect to the parent 5[*H*]-phenanthridin-6-one (IC₅₀ = 350 nM, structure **C**, Figure 1) is outlined in Table 1. Inhibitory potency of these aza derivatives was found to be largely dependent on which ring the nitrogen atom was incorporated. While the A ring aza analogues exhibited significantly lower potency than the parent 5[*H*]-phenanthridin-6-one, all C ring aza analogues demonstrated similar or slightly better potency. Inhibitory analysis of **13**, **15a**, and **15b** demonstrates the deleterious effect of a nitrogen atom within the A ring of this core. The potencies

Scheme 6^a

^a Method B. Reagents: (i) Pd(PPh₃)₄, K₂CO₃, toluene/EtOH (10:1); (ii) HNR₁R₂ (excess), DIEA, 77–90%; (iii) Raney nickel, H₂NNH₂, 36–95%; (iv) HCl or MsOH, 85–99%.

Scheme 7^a

^a Reagents: (i) Pd(PPh₃)₄, K₂CO₃, toluene/EtOH (10:1), 82%; (ii) (1) H₂/Pd/C, MeOH, (2) THF, 3 equiv of LDA, 55% overall; (iii) chloroacetyl chloride, Et₃N, DMA, 95%; (iv) HNR₂ (excess), DMA, 82–92%.

Table 1. PARP-1 Inhibition of Aza-5[*H*]-phenanthridin-6-ones

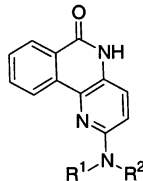
compound	name	IC ₅₀ ^b (nM)
	benzamide ^a	20000
	nicotinamide ^a	210000
C (R = H)	5[<i>H</i>]-phenanthridin-6-one	350 ± 8.9 ^c
4a	1-aza-5[<i>H</i>]-phenanthridin-6-one	116 ± 2.9 ^c
5	2-aza-5[<i>H</i>]-phenanthridin-6-one	128 ± 3.9 ^c
9	3-aza-5[<i>H</i>]-phenanthridin-6-one	169
6	4-aza-5[<i>H</i>]-phenanthridin-6-one	311
13	7-aza-5[<i>H</i>]-phenanthridin-6-one	14000
15a	8-aza-5[<i>H</i>]-phenanthridin-6-one	2600
15b	10-aza-5[<i>H</i>]-phenanthridin-6-one	2900

^a See ref 24. ^b See Experimental Section for details. ^c Represents an average of three IC₅₀ values.

of compounds **13** (IC₅₀ = 14 μM), **15a** (IC₅₀ = 2.6 μM), and **15b** (IC₅₀ = 2.9 μM) were up to an order of magnitude worse than 5[*H*]-phenanthridin-6-one, while C ring derivatives **4a**, **5**, **6**, and **9** all demonstrated similar or slightly better potency than 5[*H*]-phenanthridin-6-one. Presumably, the A ring of these aza-5[*H*]-phenanthridin-6-ones binds to the nicotinamide binding

pocket of the catalytic domain. If this holds true, the potency of **15a** can be explained by an analogous difference in potency between benzamide (IC₅₀ = 20 μM) and nicotinamide (IC₅₀ = 210 μM).²⁴ The decrease in potency for **13** and **15b** may be attributable to the ring nitrogen interacting electrostatically with residues in the hydrophobic nicotinamide binding pocket (His862, Gly863, Phe897, or Ala898). Compound **13** is the least active of these three presumably because the ring nitrogen not only interacts electrostatically with the hydrophobic binding pocket but adversely affects the hydrogen bond formed by Ser904 on the amide carbonyl. The inhibition results from the (1–4)-aza derivatives **4a**, **5**, **6**, and **9** also confirm previous findings about 5[*H*]-phenanthridin-6-one SAR,¹⁴ namely, the tolerance for hydrophilic moieties on the C ring.

While the enzymatic potencies of **4a** and **5** were slightly better than the potency of 5[*H*]-phenanthridin-6-one, preliminary stroke data on **4a** and **5** displayed significant protective effects versus 5[*H*]-phenanthridin-

Table 2. PARP-1 Inhibition of 2-Substituted 1-Aza-5[*H*]-phenanthridin-6-ones **4b–m**


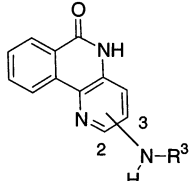
Compound	NR ² R ²	IC ₅₀ (nM)	EC ₅₀ (nM) ^c
4b		339	n.d.
4c		173	n.d.
4d	NH ₂	209	n.d.
4e ·MsOH		112 ± 5.9 ^a	135
4f ·HCl		75 ± 1.7 ^a	177
4g		45 ± 2.2 ^a	125
4h		774	n.d.
4i ·TFA ^b		42	n.d.
4j ·MsOH		58 ± 1.2 ^a	150
4k ·MsOH ^c		51	240
4l ^d		247	5800
4m ·MsOH		71 ± 3.0 ^a	145

^a Average of three IC₅₀ values. ^b Made from deprotection of **4h**. ^c Methylation product of **4i**. ^d Oxidation product of **4g**; see Scheme 8. ^e See Experimental Section for details. n.d. = not determined.

6-one (vide infra). These data prompted further derivatization of the 1-aza and/or 2-aza analogues. On the basis of previous 5[*H*]-phenanthridin-6-one SAR data,¹⁴ the 2- and 3-positions are best suited for substitution while maintaining inhibitory potency. Because of this precedent, derivatives of the 1-aza-5[*H*]-phenanthridin-6-one core **4a** were pursued, since both the 2- and 3-positions can be substituted while derivatives of **5** can only be substituted from the 3-position.

The 2-substituted derivatives **4b–m** were assayed against PARP-1, and their potencies are outlined in Table 2. The ethylenediamino derivatives **4b** and **4c** had activities that were slightly higher than the parent **4a** (IC₅₀ = 116 nM, Table 1). A slight improvement in IC₅₀ occurred with the addition of a piperazine moiety, as seen for compounds **4g**, **4j**·MsOH, and **4m**·MsOH. In fact, this activity was even maintained for the bicyclic derivatives **4i**·TFA and **4k**·MsOH. Compound **4h**, the precursor to analogues **4i**·TFA and **4k**·MsOH (IC₅₀ = 774 nM), was the least active analogue, perhaps because of the size of the butoxycarbonyl group and/or the necessity for a charged amine functionality. The hydrophilic *N*-oxide **4l** (IC₅₀ = 247 nM), a major metabolite of **4g** as discussed vide infra, was 5–6 times less potent than its unoxidized precursor **4g** (IC₅₀ = 45 nM).

An H₂O₂ cytotoxicity assay was utilized to determine the effectiveness of PARP-1 inhibitors in penetrating cells and preventing cell death.²⁵ The cells were preincubated

Table 3. PARP-1 Inhibition of 1-Aza-5[*H*]-phenanthridin-6-ones **24a–d** and **28a–d**


Compound	Substituent position	R ³ Group	IC ₅₀ (nM) ^a	EC ₅₀ (nM) ^a
4d	2	H	209	n.d.
4n	3	H	180	n.d.
24a ·HCl	2		98	2075
28a ·HCl	3		165	2630
24b ·HCl	2		150	1110
28b ·HCl	3		111	n.d.
24c ·HCl	2		142	1270
28c ·HCl	3		134	1140
24d ·HCl	2		277	n.d.
28d ·HCl	3		86	n.d.

^a See Experimental Section for details. n.d. = not determined.

with the desired PARP-1 inhibitor and consequently damaged with H₂O₂. The concentration of the inhibitor required to achieve 50% reduction in cell death is reported as EC₅₀. For the 2-amino-1-aza-5[*H*]-phenanthridin-6-ones **4e–g** and **4j**·MsOH, the cellular activities (EC₅₀) were approximately 2–5 less potent compared to the corresponding enzymatic IC₅₀ values. The one exception to this trend was *N*-oxide **4l** whose EC₅₀ was over 20 times less potent than the inhibitory constant. This result indicates that this compound, despite being a metabolite for **4g**, does not adequately penetrate into cells and is most likely not responsible for in vivo efficacy of **4g** in animal models of brain ischemia as discussed below.

The in vitro potencies of the acyl 2- and 3-substituted derivatives of **4a** are listed in Table 3. Most of these derivatives were potent against PARP-1 regardless of the size of the substituent. The bulkiest derivative **24d** (IC₅₀ = 277 nM) was only 2–3 times less potent than the most active derivatives **24a** and **28d**. Once again, the steric bulk of these derivatives underscores the versatility of the 2- and 3-positions to modulate the pharmacologic and pharmacokinetic profiles of this series.

The cellular activities for the amides **24a–d** and **28a–d**, however, were notably less potent than their respective IC₅₀ values. Compound **24b** had the most potent EC₅₀ value within the series (1110 nM), a 7-fold decrease from its IC₅₀. In addition, there is an order of magnitude difference in cellular activity between the 2- and 3-amido-1-aza-5[*H*]-phenanthridin-6-ones and the corresponding 2-substituted piperazines outlined in Table 2.

Pharmacology Data

Solubility Data. Because of the structural characteristics of most PARP-1 inhibitors (i.e., highly conjugated, crystalline, and planar), poor aqueous solubility is a significant issue. To develop a drug for acute ischemic injuries (i.e., stroke, MI), the compound should ideally be soluble in intravenous buffers (e.g., citrate,

Table 4. Solubility Measurements^a

compound	concn (mg/mL)	salt	turbidity measurement (CB ^b)	turbidity measurement (PBS ^c)
4g	5	HCl	13.0	26.8
4g	5	MsOH	1.3	1.4
4g	20	MsOH	4.0	145
4g	40	MsOH	45.7	215
4e	5	MsOH	17	pcp
4m	5	MsOH	11.5	pcp
24a	5	HCl	143	190
24c	5	HCl	12.7	17.4
24c	20	HCl	13.0	15.6
24c	40	HCl	21.0	pcp
24d	5	HCl	25.3	63.1

^a All measurements were taken on a Nepheloskan Ascent instrument, type 750, manufactured by Labsystems. Baseline reading = 0.1. Turbidity measurement greater than 20 indicates that the compound is insoluble. pcp = precipitate. ^b CB = 50 mM citrate buffer, pH = 4.0. ^c PBS = 70 mM phosphate-buffered saline solution, pH = 7.4.

Table 5. C_{\max} Values for Selected PARP-1 Inhibitors in Rats (10 mg/kg, $n = 6$)^a

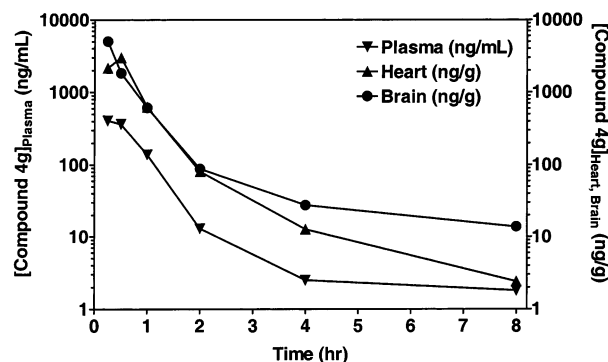
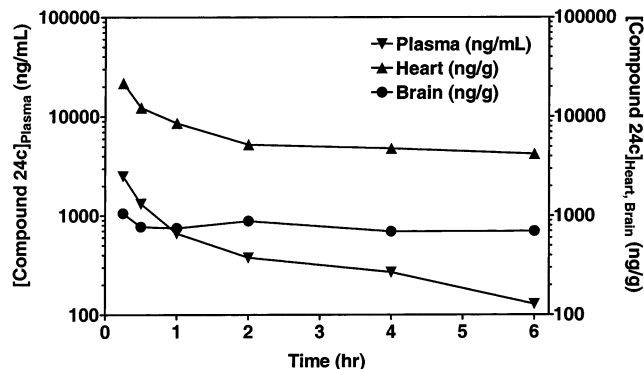
compound	C_{\max}		
	plasma ($\mu\text{g/mL}$)	heart ($\mu\text{g/g}$)	brain ($\mu\text{g/g}$)
4g ·MsOH	0.456	2.98	13.7
4m ·MsOH	1.95	7.48	8.85
24c ·HCl	4.79	38.4	1.44
4l	0.010	nd	nd
4j ·MsOH	3.79	20.3	2.18

^a Compounds were injected intravenously using 70 mM PBS as the buffer. nd = not detected.

phosphate) and deliverable by bolus injection or infusion. To determine the relative solubility of many of these analogues, turbidity measurements were taken at 5–20 mg/mL in two common buffers, namely, citrate buffer (CB) and phosphate buffered saline (PBS) (Table 4).²⁶ These solubility data acted as a guideline in determining the derivatives that could be tested as intravenous solutions in vivo and the maximum concentrations at which they could be administered. Concentrations that had turbidity measurements higher than 20 were considered insoluble and not used for administration in animal models.

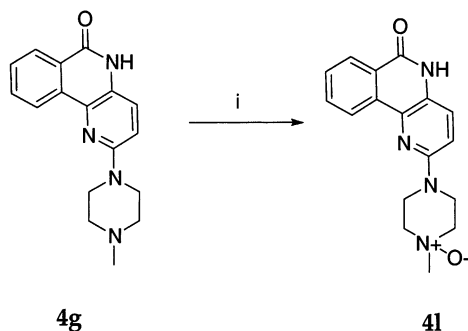
In general, most piperazine mesylate salts (**4e**·MsOH, **4g**·MsOH, and **4m**·MsOH) were soluble in the 50 mM citrate buffer at 5 mg/mL. Piperazine **4g**, one of the most soluble compounds within the series, was soluble as both the HCl and MsOH salt in CB, even though the HCl salt only had limited solubility in PBS. Compound **4g**·MsOH was the only piperazine with a high concentration limit of 20 mg/mL in citrate buffer. Of all the 2- and 3-amido derivatives tested, only compound **24c**·HCl was soluble in any buffer by turbidity measurements. The high concentration limit for amide **24c**·HCl was 20 mg/mL in CB. These parameters were eventually used as a guideline for in vivo administration in the models discussed below.

In Vivo Results. Drug Metabolism and Pharmacokinetic Data. After the aqueous solubility for the amine and amide derivatives of **4a** was established, the next logical step was to obtain drug metabolism and rat pharmacokinetic (PK) data for representative compounds from each subseries to prioritize the compounds for in vivo testing. Table 5 outlines the C_{\max} values in the plasma, heart, and brain for selected 2-substituted

**Figure 2.** Pharmacokinetic profile of **4g**·MsOH.**Figure 3.** Pharmacokinetic profile of **24c**·HCl.

1-aza-5[*H*]-phenanthridin-6-ones (administered intravenously in citrate buffer). A notable feature of these data is the structural similarity between piperazines **4g**·MsOH and **4m**·MsOH and the requisite similarities in distribution. These two compounds have the highest C_{\max} values of those tested, especially in the brain. A graphical representation of the PK profile of **4g**·MsOH is illustrated in Figure 2. There is, however, a noticeable PK profile difference between these piperazines and amide derivative **24c**·HCl (Figure 3). Namely, amide **24c**·HCl does not achieve brain levels as high as the piperazines, yet **24c**·HCl does have a much higher heart level and a much longer half-life (consequently a larger area under the curve (AUC)), as seen in the graphical depiction in Figure 3. All three compounds (**4g**·MsOH, **4m**·MsOH, and **24c**·HCl) have higher concentrations in the heart and brain than the plasma (4–30 times higher). The ability to achieve high tissue concentrations emphasizes the permeability of these PARP-1 inhibitors and could be beneficial for treating stroke and heart ischemia, given that the enzyme target (PARP-1) is tissue-based.

The PK profile for **4g**·MsOH (Figure 2) illustrates a relatively short half-life but relatively high C_{\max} in tissues. This short half-life indicates that the parent compound is rapidly metabolized in the rat, causing depletion of the parent compound. To address the metabolism issue, **4g**·MsOH was subjected to liver microsomal enzymes and the byproducts were analyzed by LC/MS. The major metabolites result from the oxidative degradation of the piperazine ring. The major product resulting from the microsomal exposure of **4g**·MsOH had a mass of 310, which corresponds to the parent compound plus one oxygen atom. Because there are multiple potential sites of oxidation, we conducted a synthetic effort to establish the most prevalent

Scheme 8^a

^a Reagents: (i) *m*CPBA, DCE, 75%, or rat microsomal enzymes.

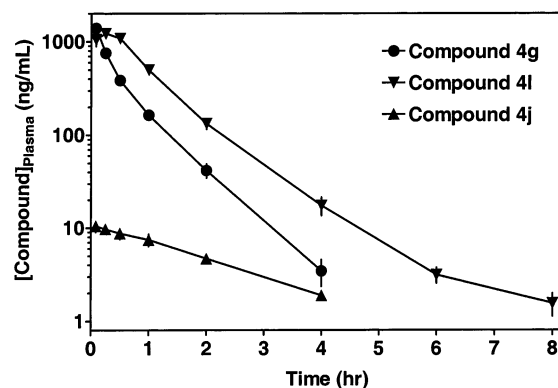
Table 6. Cerebral Ischemic Stroke Results

compound	dose (mg/kg)	<i>n</i> ^a	reduction in infarct volume (%)	MCAO model
4a	80 ^b	10	55 ($\rho = 0.055$)	transient ^d
5	40 ^b	10	47 ($\rho = 0.031$)	transient ^d
C (R = H)	40 ^b	10	-7 ($\rho = \text{ns}^f$)	transient ^d
4g ·MsOH	40 ^c	10	44 ($\rho = 0.008$)	transient ^d
4g ·MsOH	20 ^c	10	33 ($\rho = 0.017$)	transient ^d
24c ·HCl	80 ^c	10	-1 ($\rho = \text{ns}^f$)	transient ^d
4g ·MsOH	80 ^c	10	35 ($\rho = 0.039$)	permanent ^e
4g ·MsOH	40 ^c	10	18 ($\rho = 0.02$)	permanent ^e

^a *n* = number of rats per experiment. ^b Compound was administered intraperitoneally. ^c Compound was administered intravenously. ^d Half of compound was administered as a bolus dose 30 min before ischemia, and half was administered 30 min after reperfusion. See ref 31. ^e Half of compound was administered as a bolus dose 30 min before ischemia, and half was administered 30 min after ischemia. See ref 32. ^f ns = not significant.

metabolite. When compound **4g** was subjected to 1 equiv of *m*-CPBA, the major product was compound **4l**,²⁷ one potential metabolite (Scheme 8). This similar oxidation appeared to be rapidly catalyzed by either a flavin monooxygenase²⁸ or a cytochrome P450 enzyme²⁹ within the microsomal culture. Direct comparison of the microsomal culture with a pure sample of **4l** confirmed this as the major metabolite. Compound **4l** displayed a drastically different PK profile than the parent **4g**, as outlined in Table 5. This material **4l**, due to the presence of a polar *N*-oxide moiety, was not detected in the brain or heart tissue.

Another minor product from the microsomal degradation study displayed a mass of 279, corresponding to the parent compound without a methyl group. The demethyl compound **4j** was synthesized as outlined in Scheme 6 and directly compared to the microsomal samples. Compound **4j**·MsOH ($IC_{50} = 58$ nM, Table 3), whose free base is a product resulting from oxidative demethylation³⁰ of the piperazine methyl group, displayed a different PK profile than the metabolic precursor **4g**·MsOH (Table 6). That is, the C_{max} for **4j** was 6-fold lower in the brain while the C_{max} for **4j** was almost 10-fold higher in the heart than **4g**·MsOH. A graphical representation of the metabolism of **4g**·MsOH in Wistar rats is illustrated in Figure 4 (plasma only). The appearance of **4l** and, to a lesser extent, the demethyl compound **4j** proceeds immediately, presumably because of rapid oxidation or demethylation of **4g**. The rapid clearance of the piperazine **4g** happens while the two major metabolites **4j** and **4l** are detected. Once formed, **4j** and **4l** disappear at a rate similar to that of **4g**.

Figure 4. Metabolism of compound **4g** (Wistar rat).

Focal Cerebral Ischemic Stroke Data. On the basis of their solubility and pharmacokinetic profiles, compounds **4g**·MsOH and **24c**·HCl were chosen for animal brain ischemia studies. A widely accepted animal model of brain ischemia is the transient MCAO stroke model.³¹ Table 6 outlines the effects of the PARP-1 inhibitors that were tested in this model. These compounds were administered 30 min before occlusion of the middle cerebral artery and immediately after reperfusion in a bolus dose (20 or 40 mg/mL iv in CB or ip in DMSO over 3 min for **4a**, **5**, and **C**). After several hours, the stroked animals were sacrificed and brain slices were analyzed to calculate the overall area of infarction or dead tissue. Reduction in this area represents a protective effect and is noted in Table 6 as a reduction in infarct volume. The initial results for this model were obtained with the parent aza-5[*H*]-phenanthridin-6-ones **4a** and **5** via intraperitoneal administration. Compound **4a** showed a strong trend toward reduction in infarct volume when dosed at 40 mg/kg 30 min before ischemia and 40 mg/kg after reperfusion. This type of effect was mirrored by the 2-aza analogue **5**. These initial results were surprising because 5[*H*]-phenanthridin-6-one did not show protection in the same model. Clearly, the only limits to pursuing **4a** and **5** as potential drug candidates are their innate aqueous solubility and inability to be administered intravenously. For this reason, the amine salts **4g**·MsOH and **24c**·HCl were designed and synthesized to overcome these shortcomings. The results for **4g**·MsOH were very encouraging, as illustrated in Table 6. At the 40 mg/kg total dose, **4g**·MsOH resulted in a 44% reduction in infarct volume in this transient model. The majority of this protective effect was even maintained at the lower dose of 20 mg/kg. The two potential metabolites of **4g**, namely, **4j** and **4l**, are both viable inhibitors of PARP-1 and could potentially account for some of the efficacy in this MCAO model (Table 2). The pharmacokinetic analysis, however, indicates that the *N*-oxide **4l** does not penetrate readily into tissues and hence is most likely not responsible for in vivo efficacy in this model. In addition, the minimal amount of **4j** available from metabolism (2 orders of magnitude less than **4g**) indicates that **4j** is probably not responsible for the efficacy either.

Unfortunately, amide **24c**·HCl did not afford the same level of protection as **4g**·MsOH. In fact, at an 80 mg/kg total dose, **24c**·HCl did not show any reduction in infarct volume. One possible explanation for this result can be

Table 7. Rat Myocardial Ischemia Data

compound	vehicle	<i>n</i> ^a	dose ^b (mg/kg)	reduction in infarct volume (%)
4g ·MsOH	70 mM PBS	8	80	25.5 ($\rho = 0.013$)
4g ·MsOH	70 mM PBS	8	40	18.8 ($\rho = 0.08$)
4m ·MsOH	50 mM CB	8	40	36 ($\rho = 0.001$)
24c ·HCl	50 mM CB	8	80	44 ($\rho = 0.001$)
24c ·HCl	50 mM CB	8	40	39 ($\rho = 0.007$)
24c ·HCl	50 mM CB	8	20	13 ($\rho = 0.15$)

^a *n* = number of rats per experiment. ^b Half of compound was administered intravenously 5 min before ischemia and 5 min before reperfusion.

gathered from the pharmacokinetic data for these two compounds. Analogue **4g**·MsOH, while having a significantly shorter half-life than **24c**·HCl, does have a higher C_{\max} in the brain. Perhaps this high initial concentration of drug is necessary to achieve a protective effect in ischemic models such as the rat transient MCAO. This result also illustrates that C_{\max} may be a more relevant PK parameter than the half-life or AUC for predicting the protective effects of PARP-1 inhibitors in brain ischemia. That is, compound **24c**·HCl has a longer half-life (and larger AUC) in the brain than **4g**·MsOH but its C_{\max} is 10 times lower than that of **4g**·MsOH.

A more stringent animal model of brain ischemia is the rat permanent MCAO model.³² In this model, the middle cerebral artery is permanently occluded as opposed to the temporary occlusion of the transient model. Infarct volume was determined in a manner similar to the transient model, and this value is recorded in Table 6 as percent reduction in infarct volume. The PARP-1 inhibitor **4g**·MsOH was administered 30 min before ischemia at 40 mg/kg and 30 min after ischemia at 40 mg/kg and still demonstrated a significant reduction in infarct volume (35%). In fact, lowering the dose to 20 mg/kg before and 20 mg/kg after also resulted in an 18% reduction.

Myocardial Ischemia Data. If C_{\max} is also the relevant pharmacokinetic parameter for heart ischemia, one would predict that the *in vivo* efficacy of **24c**·HCl would be better in the rat model of myocardial infarction than **4g**·MsOH.^{33,34} While the brain levels for compound **4g**·MsOH are higher than those for **24c**·HCl, their relative concentrations in the heart are juxtaposed. That is, **24c**·HCl has maximum heart levels that are 13 times higher than **4g**·MsOH (Table 5). The protective results from these two compounds are outlined in Table 7. As expected, compound **4g**·MsOH displayed a modest reduction in infarct volume at the two doses tested (40 mg/kg 5' before ischemia, 40 mg/kg 5' before reperfusion) while amide **24c**·HCl, at this same dose (80 mg/kg), reduced the infarct volume by 44%. Even at the 40 mg/kg total dose, **24c**·HCl maintained efficacy (39%). Similarly, compound **4m**·MsOH displayed better protection at the 40 mg/kg dose than **4g**·MsOH, correlating with their relative C_{\max} values in the heart tissue. These *in vivo* results once again illustrate the utility of C_{\max} as a pharmacokinetic parameter to predict efficacy in an ischemic model. All together, these data indicate that PARP-1 inhibitors can potentially be used to reduce the damage caused by myocardial infarction.

Conclusions

We have designed and synthesized a series of aza-5[*H*]-phenanthridin-6-ones as potent PARP-1 inhibitors with clearly defined structure–activity relationships. These SAR studies further elucidate the hydrophobic constraints of the nicotinamide binding pocket by demonstrating the lack of activity of aza-5[*H*]-phenanthridin-6-ones **13**, **15a**, and **15b**. The aza-5[*H*]-phenanthridin-6-one core has shown *in vitro* activity similar to that of 5[*H*]-phenanthridin-6-one but has shown a notably better *in vivo* efficacy in ischemic models as displayed by compounds **4a** and **5**. Derivatization of the 1-aza-5[*H*]-phenanthridin-6-one core led to several examples of potent PARP-1 inhibitors (42–100 nM). In addition to the enzymatic activity, this series contains examples of compounds with ionizable groups for increased aqueous solubility and thus potential clinical utility in acute settings. We established C_{\max} values for selected inhibitors to predict *in vivo* efficacy in animal models of ischemia. Most importantly, we have demonstrated three 1-aza-5[*H*]-phenanthridin-6-one PARP-1 inhibitors (**4g**, **4m**, and **24c**) that are protective when administered intravenously in animal models of heart ischemia and stroke.

Experimental Section

General. Melting points were obtained on a MEL-TEMP II and were uncorrected (Meltemp Laboratory Devices, Inc.). Proton nuclear magnetic resonance were recorded at 400 MHz on a Bruker 400 using deuterated solvent as an internal standard. Chemical shift values are indicated in parts per million. Mass spectra were recorded using a Micromass LCS Platform LC/MS spectrometer. Elemental analyses were obtained from Atlantic Microlabs, Inc. (Norcross, GA). All reagents were purchased from Aldrich Chemical (Milwaukee, WI) or CB Reasearch (New Castle, DE) unless otherwise stated.

General Procedure for the Synthesis of 2-(3-Aminopyridin-2-yl)-*N,N*-diisopropylbenzamide (3a). The boronic acid **1** (2.0 g, 8.0 mmol), prepared according to the literature,¹⁹ was added to a solution of potassium carbonate (2.2 g in 8 mL of H₂O) and 2-chloro-3-amino pyridine **2a** (0.94 g, 7.3 mmol) in 100 mL of toluene/EtOH (9:1). This mixture was deoxygenated *in vacuo* and refilled with nitrogen. After the mixture was stirred under nitrogen for 30 min, palladium tetrakis(triphenylphosphine) (420 mg, 0.36 mmol) was added to the mixture. The solution was heated to 80 °C until complete conversion was attained according to TLC (50:50 hexanes/EtOAc). The solvent was removed *in vacuo*, and the reaction mixture was then partitioned between water (100 mL) and EtOAc (100 mL). The water layer was extracted two more times with EtOAc (100 mL), and the combined organic layers were dried with Na₂SO₄ and concentrated to yield a crude solid that was triturated with diethyl ether (10–20 mL) to yield the desired amine **3a** as a yellow solid (1.84 g, 85%): ¹H NMR (CDCl₃) δ 8.05 (d, 1H), 7.45 (m, 3H), 7.28 (d, 1H), 7.06 (m, 1H), 7.00 (d, 1H), 4.01 (s, 2H), 3.78 (m, 1H), 3.31 (m, 1H), 1.48 (d, 3H), 1.13 (d, 3H), 1.01 (d, 3H), 0.84 (d, 3H); MS (ES⁺) = 298. Anal. (C₁₈H₂₃N₃O) C, H, N.

2-(4-Aminopyridin-3-yl)-*N,N*-diisopropylbenzamide (3b). 4-Amino-3-iodopyridine **2b** (1.4 g, 8.1 mmol), boronic acid **1** (2.0 g, 8.9 mmol), and potassium carbonate (2.2 g, 15.9 mmol) were dissolved in 80 mL of toluene, 8 mL of EtOH, and 8 mL of H₂O. This mixture was purged of oxygen and refilled with nitrogen several times. Then, tetrakis(triphenylphosphine)palladium (350 mg, 0.30 mmol) was added to the mixture, and the mixture was heated to 80 °C overnight. Water (100 mL) was then added to the reaction mixture, and the organic layer was partitioned. The aqueous layer was extracted with EtOAc (2 × 100 mL), and the combined organics were dried with Na₂

SO₄ and concentrated. The crude reaction product was triturated with diethyl ether (25 mL) and filtered. The resulting solid was collected and characterized as the biphenylamine **3b** (2.0 g, 83%): ¹H NMR (CDCl₃) δ 8.17 (d, 1H), 8.03 (s, 1H), 7.45 (m, 2H), 7.25 (m, 2H), 6.55 (d, 1H), 4.50 (bs, 2H), 3.61 (m, 1H), 3.31 (m, 1H), 1.49 (d, 3H), 1.16 (d, 3H), 1.03 (d, 3H), 0.83 (d, 3H); MS (ES⁺) = 298. Anal. (C₁₈H₂₃N₃O) C, H, N.

2-(2-Aminopyridin-3-yl)-N,N-diisopropylbenzamide (3c). The synthesis was carried out in a manner identical to that of **3b** (73%): ¹H NMR (CDCl₃) δ 7.94 (d, 1H), 7.44 (m, 2H), 7.29 (m, 2H), 6.58 (m, 1H), 5.49 (bs, 2H), 3.56 (m, 2H), 1.40 (d, 3H), 1.05 (d, 3H), 0.93 (d, 3H), 0.64 (d, 3H). Anal. (C₁₈H₂₃N₃O) C, H, N.

1-Aza-5[H]-phenanthridin-6-one (4a). The amine **3a** (1.74 g, 5.8 mmol) was dissolved in dry tetrahydrofuran (25 mL), and the mixture was cooled to -78 °C under nitrogen. Lithium diisopropylamide (2.0 M, 7.6 mL) was added dropwise to the solution, and this mixture was stirred for several hours and warmed to room temperature overnight. The reaction was quenched with water (50 mL), and the mixture was extracted with 10% MeOH/CH₂Cl₂. The combined organics were dried and concentrated to yield the crude solid, which was triturated with boiling diethyl ether to yield the pure material **4a** as a yellow solid (0.95 g, 89%): mp = 300–320 °C (dec); ¹H NMR (DMSO-*d*₆) δ 11.78 (s, 1H), 8.77 (d, 1H), 8.55 (d, 1H), 8.32 (d, 1H), 7.93 (d, 1H), 7.74 (m, 2H), 7.54 (m, 1H); MS (ES⁺) = 197. Anal. (C₁₂H₈N₂O) C, H, N.

2-Aza-5[H]-phenanthridin-6-one (5). A solution of lithium diisopropylamide (2.0 M, 10 mL) was dissolved in 90 mL of THF, and the mixture was cooled to -78 °C. A solution of amine **3b** (2.0 g, 6.73 mmol) in THF (25 mL) was added to the LDA dropwise over a 15 min period. The reaction mixture was warmed to room temperature and stirred overnight. The reaction mixture was concentrated in vacuo and suspended in 100 mL of water. The solid was filtered off and triturated with ethyl acetate (100 mL). The resulting solid was dried to yield the desired compound **5** (1.24 g, 94%): mp = 300–320 °C (dec); ¹H NMR (DMSO-*d*₆) δ 11.57 (bs, 1H), 9.57 (s, 1H), 8.65 (d, 1H), 8.50 (d, 1H), 8.33 (d, 1H), 7.90 (t, 1H), 7.71 (t, 1H), 7.28 (d, 1H); MS (ES⁺) = 197. Anal. (C₁₂H₈N₂O) C, H, N.

4-Aza-5[H]-phenanthridin-6-one (6). The cyclization was done in a manner similar to the cyclization of amine **6** (78%): mp = 295–300 °C; ¹H NMR (DMSO-*d*₆) δ 12.05 (bs, 1H), 8.84 (d, 1H), 8.53 (d, 1H), 8.51 (d, 1H), 8.34 (d, 1H), 7.91 (t, 1H), 7.71 (t, 1H), 7.34 (m, 1H); MS (ES⁺) = 197. Anal. (C₁₂H₈N₂O) C, H, N.

2-[3-(2,2-Dimethylpropionylamino)pyridin-4-yl]-N,N-diisopropylbenzamide (8). Boronic acid **1** (1.3 g, 5.2 mmol) and 2,2-dimethyl-*N*-(4-iodo-3-pyridinyl)propanamide (700 mg, 2.3 mmol) **7** were dissolved in DME (25 mL). Tetrakis(triphenylphosphine)palladium (133 mg, 0.11 mmol) and 2 M sodium carbonate solution (2.2 mL) were added. The reaction mixture was refluxed at 83 °C for 18 h. The mixture was concentrated in vacuo, extracted with EtOAc, washed with brine, and dried with sodium sulfate. The crude oil was chromatographed (CH₂Cl₂, 1–5% MeOH/CH₂Cl₂) to obtain **8** as a white solid (503 mg, 57%): ¹H NMR (DMSO-*d*₆) δ 9.08 (s, 1H), 8.64 (s, 1H), 8.43 (d, 1H), 7.58–7.48 (m, 2H), 7.40 (dd, 1H), 7.33 (d, 1H), 7.24 (dd, 1H), 3.53–3.36 (m, 2H), 1.38 (d, 3H), 1.01 (d, 3H), 0.97 (s, 9H), 0.91 (d, 3H), 0.77 (d, 3H); MS (ES⁺) = 382.0. Anal. (C₂₃H₃₁N₃O) C, H, N.

3-Aza-5[H]-phenanthridin-6-one (9). Amide **8** (485 mg, 1.27 mmol) was dissolved in methanol (20 mL). Concentrated HCl (1 mL) was added, followed by 24 h of refluxing of the mixture. A white solid that precipitated out of solution was filtered and dissolved in H₂O. After 15 min of stirring, the free base crashed out of solution. The solid was filtered and dried, providing 150 mg of the desired final product **9** as a white solid (60%): mp = 303–309 °C; ¹H NMR (DMSO-*d*₆) δ 8.70 (s, 1H), 8.60 (d, 1H), 8.41 (t, 2H), 8.31 (d, 1H), 7.95 (t, 1H), 7.80 (t, 1H); MS (ES⁺) = 197. Anal. (C₁₂H₈N₂O·0.3H₂O) C, H, N.

5,6-Dihydrobenzo[*f*][1,7]naphthyridin-5-ylamine (12). The boronic acid **11** (1.1 g, 4.6 mmol), prepared according to the literature method,²³ 2-cyano-3-bromopyridine (770 mg, 4.2

mmol), potassium carbonate (1 g, 7.25 mmol), and tetrakis(triphenylphosphine)palladium (100 mg, catalyst) were mixed together in toluene (50 mL) and ethanol (5 mL) and heated to 70 °C overnight. The reaction was quenched with water (75 mL), and the mixture was then extracted with EtOAc (3 × 50 mL). The combined organics were dried and concentrated in vacuo and chromatographed (50:50 EtOAc/hexanes to 10% MeOH/EtOAc) to yield the amine **12** (235 mg, 29%): mp = 294–298 °C; ¹H NMR (DMSO-*d*₆) δ 8.86 (d, 1H), 8.75 (d, 1H), 8.28 (d, 1H), 7.72 (m, 2H), 7.61 (t, 1H), 7.38 (t, 1H), 6.21 (bs, 2H); MS (ES⁺) = 196. Anal. (C₁₂H₉N₃) C, H, N.

7-Aza-5[H]-phenanthridin-6-one (13). The aniline **12** (50 mg, 0.25 mmol) was suspended in 1 mL of H₂O and 0.7 mL of H₂SO₄ and cooled to 0 °C. A solution of NaNO₂ (18 mg, 0.26 mmol in 0.2 mL of H₂O) was added to the acidic solution dropwise. The reaction mixture was warmed to room temperature and heated to 100 °C for 3 h. The mixture was then cooled to room temperature, and some particulates were filtered off. The filtrate was set out overnight, and the resulting crystals were filtered off and triturated with boiling EtOAc and filtered. The resulting solid was characterized as the desired material **13** (11.2 mg, 22%): mp = 300–310 °C; ¹H NMR (DMSO-*d*₆) δ 11.91 (s, 1H), 8.98 (d, 1H), 8.43 (d, 1H), 7.85 (m, 1H), 7.55 (m, 2H), 7.38 (m, 2H); MS (ES⁺) = 197. Anal. (C₁₂H₈N₂O) C, H, N.

8-Aza-5[H]-phenanthridin-6-one (15a). 4-Chloronicotinic acid ethyl ester **14a** (500 mg, 2.7 mmol), boronic acid **10** (1.5 g, 6.1 mmol), sodium carbonate (715 mg, 6.6 mmol), and tetrakis(triphenylphosphine)palladium (140 mg, catalyst) were suspended in DME (30 mL) and heated to 80 °C overnight. The solvent was removed in vacuo and the residue was chromatographed on silica gel (50% EtOAc/hexanes to 10% MeOH/EtOAc) to yield the desired compound **15a** as a yellow solid (124 mg, 24%): mp = 295–300 °C; ¹H NMR (DMSO-*d*₆) δ 11.80 (bs, 1H), 9.43 (s, 1H), 8.91 (d, 1H), 8.43 (m, 2H), 7.62 (t, 1H), 7.32 (m, 2H); MS (ES⁺) = 197. Anal. (C₁₂H₈N₂O) C, H, N.

10-Aza-5[H]-phenanthridin-6-one (15b). The same procedure was used as **15a** with boronic ester **10** and 2-chloropicolinic acid ethyl ester **14b** to afford **15b** as a yellow solid (34%): mp = 295–300 °C; ¹H NMR (DMSO-*d*₆) δ 11.90 (bs, 1H), 9.06 (d, 1H), 8.63 (m, 2H), 7.69 (m, 1H), 7.60 (t, 1H), 7.40 (d, 1H), 7.32 (m, 1H); MS (ES⁺) = 197. Anal. (C₁₂H₈N₂O) C, H, N.

Method A. Synthesis of 2-(6-Chloro-3-nitropyridin-2-yl)-N,N-diisopropylbenzamide (17a). The boronic acid **1** (2.0 g, 8.0 mmol) was added to a solution of potassium carbonate (2.2 g in 8 mL of H₂O) and 2,5-dichloro-3-nitropyridine **16** (1.4 g, 7.3 mmol) in 100 mL of toluene/EtOH (8:1). This mixture was deoxygenated in vacuo and refilled with nitrogen. After the mixture was stirred under nitrogen for 30 min, tetrakis(triphenylphosphine)palladium (250 mg) was added to the mixture. The solution was heated to 80 °C until complete conversion (no starting material) according to TLC (50:50 hexanes/EtOAc). The reaction mixture was then extracted with water and the toluene layer was dried and concentrated to yield a crude oil that was columned on silica gel to afford the desired isomer **17a** as a yellow oil (1.20 g, 42%): ¹H NMR (CDCl₃) δ 8.26 (d, 1H), 7.45 (m, 3H), 7.34 (m, 2H), 3.99 (m, 1H), 3.41 (m, 1H), 1.38 (bs, 9H), 1.21 (d, 3H); MS (ES⁺) = 363. Anal. (C₁₈H₂₀ClN₃O₃) C, H, N.

This material was carried on to the cyclization without further characterization. The undesired isomer **17b** was also isolated as a yellow oil (1.01 g, 38%): ¹H NMR (CDCl₃) δ 8.26 (d, 1H), 7.45 (m, 4H), 7.34 (t, 1H), 3.99 (m, 1H), 3.41 (m, 1H), 1.37 (bs, 6H), 1.21 (d, 6H); MS (ES⁺) = 363. Anal. (C₁₈H₂₀ClN₃O₃) C, H, N.

General Procedure for the Synthesis of Nitroamines 18b–g. Chloride **17a** (300 mg, 0.83 mmol) was dissolved in THF (5 mL) followed by the addition of diisopropylethylamine (160 μL, 0.91 mmol) and 2-(4-aminoethyl)morpholine (220 μL, 1.66 mmol). The reaction mixture was heated to 65 °C overnight, and TLC analysis indicated a low running spot on the baseline (EtOAc). Water (5 mL) was added to the mixture

followed by extraction with CH_2Cl_2 (3×10 mL). The combined organics were dried and concentrated in vacuo to yield a crude foam that solidified upon drying in vacuo. The solid was triturated with hexanes and filtered to yield the desired amine **18b** (320 mg, 85%).

***N,N*-Diisopropyl-2-[6-(2-morpholin-4-ylethylamino)-3-nitropyridin-2-yl]benzamide (18b)**: yield = 85%; ^1H NMR ($\text{DMSO}-d_6$) δ 8.21 (m, 1H), 7.40 (m, 5H), 6.36 (d, 1H), 3.97 (m, 1H), 3.70 (m, 6H), 3.47 (m, 2H), 3.31 (m, 1H), 2.45 (m, 6H), 1.48 (bs, 3H), 1.24 (bs, 3H), 1.06 (bs, 3H), 0.87 (bs, 3H); MS (ES^+) = 456. Anal. ($\text{C}_{24}\text{H}_{33}\text{N}_5\text{O}_4$) C, H, N.

2-[6-(2-Diethylaminoethylamino)-3-nitropyridin-2-yl]-*N,N*-diisopropylbenzamide (18c): yield = 92%; ^1H NMR (CDCl_3) δ 8.15 (d, 1H), 7.39 (m, 3H), 7.30 (m, 1H), 6.26 (d, 1H), 3.96 (bs, 1H), 3.50 (bs, 1H), 3.30 (m, 1H), 2.53 (m, 3H), 1.86 (bs, 1H), 1.71 (m, 2H), 1.48 (bs, 3H), 1.35 (bs, 3H), 1.04 (t, 10H), 0.76 (bs, 3H). MS (ES^+) = 442. Anal. ($\text{C}_{25}\text{H}_{37}\text{N}_5\text{O}_3$) C, H, N.

2-(6-Amino-3-nitropyridin-2-yl)-*N,N*-diisopropylbenzamide (18d): yield = 72%; ^1H NMR (CDCl_3) δ 8.15 (d, 1H), 7.42 (m, 2H), 7.33 (m, 2H), 6.42 (d, 1H), 5.32 (s, 2H), 3.95 (m, 1H), 3.33 (m, 1H), 1.43 (bs, 6H), 0.99 (bs, 6H). MS (ES^+) = 343. Anal. ($\text{C}_{18}\text{H}_{22}\text{N}_4\text{O}_3$) C, H, N.

***N,N*-Diisopropyl-2-[6-(4-isopropylpiperazin-1-yl)-3-nitropyridin-2-yl]benzamide (18e)**: yield = 83%; ^1H NMR (CDCl_3) δ 8.19 (d, 1H), 7.33–7.43 (m, 2H), 7.25 (bs, 1H), 6.51 (d, 1H), 3.97 (bs, 1H), 3.76 (s, 4H), 3.28 (m, 1H), 2.71 (m, 1H), 2.58 (t, 4H), 1.48 (s, 3H), 1.22 (s, 3H), 1.04 (d, 6H), 1.00 (s, 3H), 0.67 (s, 3H). MS (ES^+) = 454. Anal. ($\text{C}_{25}\text{H}_{35}\text{N}_5\text{O}_3$) C, H, N.

***N,N*-Diisopropyl-2-(5'-nitro-4-pyrrolidin-1-yl-3,4,5,6-tetrahydro-2H-[1,2']bipyridinyl-6'-yl)benzamide (18f)**: yield = 81%; ^1H NMR (CDCl_3) δ 8.17 (d, 1H), 7.40 (m, 3H), 7.27 (m, 1H), 6.65 (d, 1H), 4.45 (bs, 1H), 3.97 (bs, 1H), 3.27 (m, 1H), 3.05 (t, 2H), 2.58 (s, 5H), 2.25 (m, 1H), 1.98 (d, H), 1.79 (s, 5H), 1.50 (m, 6H), 1.21 (bs, 3H), 1.00 (bs, 3H), 0.67 (bs, 3H). MS (ES^+) = 426. Anal. ($\text{C}_{27}\text{H}_{37}\text{N}_5\text{O}_3 \cdot 0.5\text{H}_2\text{O}$) C, H, N.

***N,N*-Diisopropyl-2-[6-(4-methylpiperazin-1-yl)-3-nitropyridin-2-yl]benzamide (18g)**: yield = 83%; ^1H NMR (CDCl_3) δ 8.19 (d, 1H), 7.34–7.46 (m, 3H), 7.25 (m, 1H), 6.53 (d, 1H), 3.97 (s, 1H), 3.76 (bs, 4H), 3.28 (m, 1H), 2.47 (t, 4H), 2.33 (s, 3H), 1.48 (bs, 3H), 1.22 (bs, 3H), 1.00 (bs, 3H), 0.68 (bs, 3H); MS (ES^+) = 426. Anal. ($\text{C}_{23}\text{H}_{31}\text{N}_5\text{O}_3$) C, H, N.

General Procedure for the Synthesis of Anilines 19b–g. Nitro compound **18b** (300 mg, 0.66 mmol) was dissolved in MeOH (20 mL) with Pd/C (100 mg), and the mixture was hydrogenated at 30 psi for 2 h. TLC indicated complete conversion of the nitro compound (10% MeOH/EtOAc). The reaction mixture was filtered through a plug of Celite, and the filtrate was concentrated and dried. The crude foam was used in the cyclization step without further purification (275 mg, 99%): ^1H NMR (CDCl_3) δ 7.41 (m, 3H), 6.98 (d, 1H), 6.31 (d, 1H), 4.75 (bs, 2H), 3.78 (m, 1H), 3.70 (m, 4H), 3.28 (m, 3H), 2.56 (m, 2H), 2.47 (m, 4H), 1.50 (d, 3H), 1.19 (d, 3H), 1.00 (d, 3H), 0.83 (d, 3H); MS (ES^+) = 426. Anal. ($\text{C}_{24}\text{H}_{35}\text{N}_5\text{O}_2$) C, H, N.

2-[3-Amino-6-(2-diethylaminoethylamino)pyridin-2-yl]-*N,N*-diisopropylbenzamide (19c): yield = 92%; ^1H NMR (CDCl_3) δ 7.42 (m, 3H), 7.26 (m, 2H), 6.96 (d, 1H), 6.33 (d, 1H), 3.75 (m, 1H), 3.23 (m, 3H), 2.53 (m, 7H), 1.74 (m, 4H), 1.48 (d, 3H), 1.26 (s, 6H), 1.16 (d, 3H), 1.02 (m, 6H), 0.82 (m, 6H); MS (ES^+) = 412. Anal. ($\text{C}_{25}\text{H}_{39}\text{N}_5\text{O}_1 \cdot 1.8\text{MeOH}$) C, H, N.

2-(3,6-Diaminopyridin-2-yl)-*N,N*-diisopropylbenzamide (19d): yield = 89%; ^1H NMR (CDCl_3) δ 7.43 (m, 3H), 7.28 (m, 1H), 6.98 (d, 1H), 6.45 (d, 1H), 4.07 (bs, 2H), 3.78 (m, 1H), 3.32 (m, 1H), 1.50 (d, 3H), 1.19 (d, 3H), 1.01 (d, 3H), 0.89 (d, 3H). Anal. ($\text{C}_{18}\text{H}_{24}\text{N}_4\text{O} \cdot 0.5\text{C}_4\text{H}_8\text{O}_2 \cdot 0.5\text{H}_2\text{O}$) C, H, N.

2-[3-Amino-6-(4-isopropylpiperazin-1-yl)pyridin-2-yl]-*N,N*-diisopropylbenzamide (19e): yield = 98%; ^1H NMR (CDCl_3) δ 7.42 (m, 3H), 7.28 (d, 1H), 6.96 (d, 1H), 6.56 (d, 1H), 3.68 (m, 1H), 3.35 (m, 5H), 2.63 (m, 5H), 1.46 (d, 3H), 1.15 (d, 3H), 1.08 (d, 3H), 0.95 (d, 3H), 0.68 (d, 3H); MS (ES^+) = 424. Anal. ($\text{C}_{25}\text{H}_{37}\text{N}_5\text{O} \cdot 0.7\text{C}_4\text{H}_8\text{O}_2$) C, H, N.

2-(5'-Amino-4-pyrrolidin-1-yl-3,4,5,6-tetrahydro-2H-[1,2']bipyridinyl-6'-yl)-*N,N*-diisopropylbenzamide (19f): yield = 95%; ^1H NMR (CDCl_3) δ 7.42 (m, 3H), 7.28 (m, 1H), 6.98 (d, 1H), 6.60 (d, 1H), 4.09 (m, 3H), 3.69 (m, 1H), 3.27 (m, 1H), 2.66 (m, 6H), 2.17 (bs, 1H), 1.98 (bd, 2H), 1.82 (s, 4H), 1.61 (m, 2H), 1.49 (d, 3H), 1.17 (d, 3H), 0.98 (d, 3H), 0.73 (d, 3H); MS (ES^+) = 448. Anal. ($\text{C}_{18}\text{H}_{20}\text{N}_4\text{O}_5 \cdot 0.25\text{C}_4\text{H}_8\text{O}_2 \cdot 0.5\text{H}_2\text{O}$) C, H, N.

2-[3-Amino-6-(4-methylpiperazin-1-yl)pyridin-2-yl]-*N,N*-diisopropylbenzamide (19g): yield = 89%; ^1H NMR (CDCl_3) δ 7.42 (m, 3H), 7.26 (m, 2H), 6.97 (d, 1H), 6.57 (d, 1H), 3.68 (m, 1H), 3.37 (m, 7H), 2.51 (t, 4H), 2.33 (s, 3H), 1.48 (d, 3H), 1.15 (d, 3H), 0.96 (d, 3H), 0.68 (d, 3H); MS (ES^+) = 396. Anal. ($\text{C}_{23}\text{H}_{33}\text{N}_5\text{O} \cdot \text{C}_4\text{H}_8\text{O}_2$) C, H, N.

General Procedure for the Cyclization of Anilines 19b–g. The crude aniline **19b** (270 mg, 0.64 mmol) was dissolved in THF (20 mL) and cooled to -78 °C. A 2.0 M solution of LDA (1 mL) was added to the aniline, and the reaction mixture was slowly warmed to room temperature overnight. The mixture was quenched with water (10 mL) and extracted several times with EtOAc (3×15 mL). The combined organics were dried and concentrated and the resulting solid was triturated with EtOAc (3 mL) and filtered, yielding the desired amine **4b** (125 mg, 58%).

2-(2-Morpholin-4-ylethylamino)-5H-benzo[c][1,5]-naphthyridin-6-one (4b): yield = 58%; mp = 250–255 °C; ^1H NMR ($\text{DMSO}-d_6$) δ 11.46 (s, 1H), 8.70 (d, 1H), 8.32 (d, 1H), 7.92 (t, 1H), 7.71 (t, 1H), 7.49 (d, 1H), 6.82 (d, 1H), 6.63 (t, 1H), 3.66 (m, 4H), 3.58 (m, 2H), 2.60 (m, 4H); MS (ES^+) = 325. Anal. ($\text{C}_{18}\text{H}_{20}\text{N}_4\text{O}_2 \cdot 0.5\text{H}_2\text{O}$) C, H, N.

2-(2-Diethylaminoethylamino)-5H-benzo[c][1,5]-naphthyridin-6-one (4c): yield = 45%; mp = 114–116 °C; ^1H NMR ($\text{DMSO}-d_6$) δ 11.40 (s, 1H), 8.83 (d, 1H), 8.24 (d, 1H), 7.84 (t, 1H), 7.65 (t, 1H), 7.41 (d, 1H), 6.70 (d, 1H), 3.39 (m, 2H), 2.49 (m, 6H), 1.72 (m, 2H), 0.96 (t, 6H); MS (ES^-) = 233. Anal. ($\text{C}_{19}\text{H}_{24}\text{N}_4\text{O} \cdot 0.2\text{H}_2\text{O}$) C, H, N.

2-Amino-5H-benzo[c][1,5]naphthyridin-6-one (4d): yield = 75%; mp = 310–315 °C; ^1H NMR ($\text{DMSO}-d_6$) δ 11.42 (s, 1H), 8.50 (d, 1H), 8.26 (d, 1H), 7.85 (t, 1H), 7.66 (t, 1H), 7.44 (d, 1H), 7.70 (d, 1H), 6.02 (d, 2H); MS (ES^+) = 212. Anal. ($\text{C}_{12}\text{H}_9\text{N}_3\text{O} \cdot 0.10\text{C}_4\text{H}_8\text{O}_2$) C, H, N.

2-(4-Isopropylpiperazin-1-yl)-5H-benzo[c][1,5]naphthyridin-6-one (4e): yield = 57%; mp = 260–264 °C; ^1H NMR ($\text{DMSO}-d_6$) δ 11.48 (s, 1H), 8.63 (d, 1H), 8.25 (d, 1H), 7.86 (t, 1H), 7.67 (t, 1H), 7.53 (d, 1H), 7.10 (d, 1H), 3.55 (t, 4H), 2.68 (m, 1H), 2.56 (t, 4H), 1.00 (d, 6H); MS (ES^+) = 323. Anal. ($\text{C}_{19}\text{H}_{24}\text{N}_4\text{O}$) C, H, N.

2-(4-Pyrrolidin-1-ylpiperidin-1-yl)-5H-benzo[c][1,5]naphthyridin-6-one hydrochloride (4f·HCl): yield = 52%; mp = 170–175 °C; ^1H NMR (D_2O) δ 7.89 (d, 1H), 7.80 (d, 1H), 7.54 (t, 1H), 7.43 (t, 1H), 6.94 (d, 1H), 6.54 (d, 1H), 4.08 (d, 2H), 3.63 (t, 2H), 3.31 (m, 1H), 3.13 (m, 2H), 2.70 (t, 2H), 2.11–2.2 (m, 4H), 1.94 (q, 2H), 1.63 (q, 2H). Anal. ($\text{C}_{21}\text{H}_{24}\text{N}_4\text{O} \cdot 1\text{H}_2\text{O} \cdot 1.4\text{HCl}$) C, H, N.

2-(4-Methylpiperazin-1-yl)-5H-benzo[c][1,5]naphthyridin-6-one (4g): yield = 45%; mp = 283–285 °C; ^1H NMR (CDCl_3) δ 11.50 (s, 1H), 8.65 (d, 1H), 8.27 (d, 1H), 7.88 (t, 1H), 7.69 (t, 1H), 7.56 (d, 1H), 7.14 (d, 1H), 3.56 (t, 4H), 2.46 (t, 4H), 2.24 (s, 3H). MS (ES^+) = 295. Anal. ($\text{C}_{17}\text{H}_{18}\text{N}_4\text{O}$) C, H, N.

General Procedure for Salt Formation (4g·MsOH). The free base **4g** (1.0 g, 3.4 mmol) was suspended in hot THF (200 mL) followed by the addition of methanesulfonic acid (326 mg, 3.4 mmol). Stirring was continued overnight, and the resulting solid was collected by vacuum filtration and dried in vacuo to yield the mesylate salt **4g·MsOH** (1.28 g, 97%): ^1H NMR (D_2O) δ 7.74 (d, 2H), 7.48 (t, 1H), 7.40 (t, 1H), 6.78 (d, 1H), 6.37 (d, 1H), 4.09 (d, 2H), 3.55 (d, 2H), 3.08 (t, 2H), 2.92–2.96 (m, 5H), 2.74 (s, 3H). Anal. ($\text{C}_{17}\text{H}_{18}\text{N}_4\text{O} \cdot \text{MsOH}$) C, H, N.

Method B. Synthesis of 2-(6-Chloro-3-nitropyridin-2-yl)benzoic Acid Ethyl Ester (21a). The boronic ester **20** (16.0 g, 61.0 mmol), dichloronitropyridine **16** (11.7 g, 61 mmol), and potassium carbonate (21 g, 152 mmol) were dissolved in toluene/EtOH (20:1, 300 mL). This mixture was purged of oxygen and refilled several times with nitrogen. Then, tet-

rakistriphenylphosphinepalladium (~2 g) was added followed by heating the mixture to 80 °C overnight. The reaction mixture was then concentrated in vacuo and partitioned between EtOAc (200 mL) and H₂O (200 mL). The organic layer was dried with sodium sulfate and concentrated in vacuo. The crude residue was chromatographed using a gradient system (5% EtOAc/hexanes to 20% EtOAc/hexanes). The final product **21a** (*R_f* = 0.3, 10% EtOAc/hexanes) was isolated as a low-melting solid/foam (8.40 g, 45%): ¹H NMR (CDCl₃) δ 8.40 (d, 1H), 8.14 (d, 1H), 7.65 (t, 1H), 7.55 (m, 2H), 7.32 (d, 1H), 4.16 (q, 2H), 1.19 (t, 3H); MS (ES⁺) = 307. Anal. (C₁₄H₁₁ClN₂O₄) C, H, N. The undesired isomer **21b** (*R_f* = 0.2, 10% EtOAc/hexanes) was also isolated (6.9 g, 35%): ¹H NMR (CDCl₃) δ 8.32 (d, 1H), 7.92 (d, 1H), 7.56 (m, 4H), 4.25 (dd, 2H), 1.21 (t, 3H); MS (ES⁺) = 307. Anal. (C₁₄H₁₁ClN₂O₄) C, H, N.

Synthesis of 2-[6-(4-Methylpiperazin-1-yl)-3-nitropyridin-2-yl]benzoic Acid Ethyl Ester (22a). The chloride **21a** (7.12 g, 23.2 mmol) was dissolved in THF (250 mL). Diisopropylethylamine (3.3 g, 25.5 mmol) was added to this solution followed by *N*-methylpiperazine (4.6 g, 46.4 mmol). This mixture was heated to 60 °C overnight until complete conversion of the chloride was evident by TLC (*R_f* of diamine = 0.1, EtOAc). The reaction was worked up by removal of THF and partitioning between water (200 mL) and CH₂Cl₂ (200 mL). After two more extractions with CH₂Cl₂ (2 × 100 mL), the organic layer was dried with sodium sulfate and concentrated in vacuo to yield the crude diamine **22a** as a yellow oil (6.56 g, 77%): ¹H NMR (CDCl₃) δ 8.32 (d, 1H), 8.07 (d, 1H), 7.58 (t, 1H), 7.48 (t, 1H), 7.26 (d, 1H), 6.60 (d, 1H), 4.13 (q, 2H), 3.73 (t, 4H), 2.46 (t, 4H), 2.33 (s, 3H), 1.13 (t, 3H). MS (ES⁺) = 371. Anal. (C₁₉H₂₂N₄O₄) C, H, N.

2-(3-Nitro-6-piperazin-1-ylpyridin-2-yl)benzoic Acid Ethyl Ester (22b): yellow oil; yield = 90%; ¹H NMR (CDCl₃) δ 8.32 (d, 1H), 8.07 (d, 1H), 7.58 (t, 1H), 7.48 (t, 1H), 7.25 (d, 1H), 6.60 (d, 1H), 4.14 (dd, 2H), 3.72 (m, 4H), 2.97 (m, 2H), 2.57 (m, 2H), 2.50 (bs, 1H), 1.13 (t, 3H); MS (ES⁺) = 357. Anal. (C₁₈H₂₀N₄O₄) C, H, N.

(S,S)-5-[6-(2-Ethoxycarbonylphenyl)-5-nitropyridin-2-yl]-2,5-diazabicyclo[2.2.1]heptane-2-carboxylic acid *tert*-butyl ester (22c): yellow oil; yield = 82%; ¹H NMR (CDCl₃) δ 8.34 (d, 1H), 8.09 (d, 1H), 7.58 (t, 1H), 7.51 (t, 1H), 7.25 (d, 1H), 6.29 (d, 1H), 4.71 (m, 1H), 4.56 (m, 1H), 4.13 (dd, 2H), 3.54 (m, 2H), 3.40 (m, 2H), 1.91 (m, 2H), 1.43 (s, 9H), 1.14 (t, 3H); MS (ES⁺) = 469. Anal. (C₂₄H₂₈N₄O₆) C, H, N.

2-[6-(4-Cyclopropylmethylpiperazin-1-yl)-3-nitropyridin-2-yl]benzoic acid ethyl ester (22d): yellow oil; yield = 83%; ¹H NMR (CDCl₃) δ 8.32 (d, 1H), 8.08 (d, 1H), 7.58 (t, 1H), 7.48 (t, 1H), 7.25 (d, 1H), 6.60 (d, 1H), 4.13 (dd, 2H), 3.75 (m, 4H), 2.58 (m, 4H), 2.30 (m, 2H), 1.12 (t, 3H), 0.87 (m, 1H), 0.53 (m, 2H), 0.10 (m, 2H); MS (ES⁺) = 411. Anal. (C₂₂H₂₆N₄O₄) C, H, N.

Reduction/Cyclization To Form 4g. The crude diamine **22a** was dissolved in MeOH (300 mL). Wet Raney nickel was added (500 mg, catalytic amount) followed by dropwise addition of hydrazine hydrate (4.1 g, 82 mmol). The mixture was heated to reflux and monitored by TLC until completion (approximately 3 h). The product *R_f* value was 0.1 in 10% MeOH/EtOAc. The Raney nickel was then filtered off, the filtrate was concentrated, and the solid that resulted was filtered off and triturated with 50 mL of CH₃CN and filtered. The resulting light-yellow solid was dried under high vacuum for 2 h to yield **4g** (4.1 g, 84%). This material was spectroscopically identical to the product isolated from method A.

(S,S)-5-(6-Oxo-5,6-dihydrobenzo[c][1,5]naphthyridin-2-yl)-2,5-diazabicyclo[2.2.1]heptane-2-carboxylic acid *tert*-butyl ester (4h): yield = 36%; mp = 259–261 °C; ¹H NMR (DMSO-*d*₆) δ 11.44 (s, 1H), 8.65 (d, 1H), 8.26 (d, 1H), 7.67 (t, 1H), 7.45 (d, 1H), 6.85 (t, 1H), 4.92 (dd, 2H), 3.38 (m, 2H), 3.30 (s, 1H), 3.23 (m, 1H), 1.96 (d, 2H), 1.60 (s, 9H). Anal. (C₂₂H₂₄N₄O₃) C, H, N.

(S,S)-2-(2,5-Diazabicyclo[2.2.1]hept-2-yl)-5H-benzo[c][1,5]naphthyridin-6-one trifluoroacetate (4i-TFA). This compound was made by the deprotection of the Boc group of compound **4e** by 10% TFA/DCM (16 h). Removal of the solvent

afforded the TFA salt of **4i** as an off-white solid (98%): mp = 160–165 °C; ¹H NMR (DMSO-*d*₆) δ 11.54 (s, 1H), 8.68 (d, 1H), 8.59 (d, 1H), 7.90 (t, 1H), 7.72 (t, 1H), 7.61 (d, 1H), 6.92 (d, 1H), 5.04 (s, 1H), 4.53 (s, 1H), 3.68 (m, 2H), 3.29 (m, 2H), 2.19 (d, 1H), 2.00 (d, 1H). Anal. (C₁₇H₁₆N₄O·1.1TFA·0.4H₂O) C, H, N.

2-Piperazin-1-yl-5H-benzo[c][1,5]naphthyridin-6-one (4j): yield = 95%; mp = 250–252 °C; ¹H NMR (DMSO-*d*₆) δ 11.56 (s, 1H), 8.93 (bs, 1H), 8.65 (d, 1H), 8.27 (d, 1H), 7.87 (t, 1H), 7.70 (t, 1H), 7.61 (d, 1H), 7.21 (d, 1H), 3.61 (t, 4H), 3.26 (bs, 4H). Anal. (C₁₆H₁₆N₄O·0.5H₂O) C, H, N.

(S,S)-2-(5-Methyl-2,5-diazabicyclo[2.2.1]hept-2-yl)-5H-benzo[c][1,5]naphthyridin-6-one mesylate (4k·MsOH). This compound was made by alkylation of compound **4j** as described in the literature.³⁵ Salt formation was performed by suspending the free base (100 mg, 0.32 mmol) in THF (20 mL) followed by the addition of MsOH (35 mg, 0.36 mmol). The resulting salt precipitated out and was collected by filtration (110 mg, 26% overall): ¹H NMR (D₂O) δ 8.19 (d, 1H), 8.01 (d, 1H), 7.71 (t, 1H), 7.59 (t, 1H), 7.18 (d, 1H), 6.48 (d, 1H), 4.88 (m, 1H), 4.46 (m, 1H), 3.69 (m, 2H), 3.34 (m, 2H), 2.97 (s, 3H), 2.79 (s, 3H), 2.38 (m, 2H). Anal. (C₁₇H₁₆N₄O·1.1MsOH·0.4H₂O) C, H, N.

2-(4-Methyl-4-oxypiperazin-1-yl)-5H-benzo[c][1,5]naphthyridin-6-one (4l). This compound was synthesized by oxidation of **4g** (200 mg, 0.68 mmol) with *m*CPBA (235 mg, 1.0 mmol) in dichloroethane. After the mixture was stirred overnight, the solid that precipitated out was filtered off, dissolved in water (5 mL), and extracted with EtOAc (3 × 10 mL). The aqueous layer was acidified with citric acid and extracted again with EtOAc (3 × 10 mL) to remove traces of *m*-chlorobenzoic acid. The remaining aqueous layer was concentrated down, and the desired *N*-oxide **4l** precipitated out and was collected by filtration (158 mg, 75%): mp = 300–320 °C (dec); ¹H NMR (D₂O) δ 7.63 (d, 1H), 7.53 (d, 1H), 7.32 (m, 2H), 6.60 (d, 1H), 6.16 (d, 1H), 3.79 (m, 4H), 3.60 (t, 2H), 3.55 (s, 3H), 3.08 (t, 2H); MS (ES⁺) = 311. Anal. (C₁₇H₁₈N₄O₂·0.4H₂O) C, H, N.

2-(4-Cyclopropylmethylpiperazin-1-yl)-5H-benzo[c][1,5]naphthyridin-6-one mesylate (4m·MsOH): yield = 82%; ¹H NMR (D₂O) δ 8.55 (d, 1H), 8.17 (d, 1H), 7.76 (t, 1H), 7.58 (t, 1H), 7.46 (d, 1H), 7.05 (d, 1H), 3.49 (m, 4H), 2.40 (m, 4H), 2.12 (m, 2H), 0.77 (m, 1H), 0.39 (m, 2H), 0.00 (m, 2H). Anal. (C₂₀H₂₂N₄O·1.15MsOH·0.7H₂O) C, H, N.

Procedure for Synthesizing Chloroacetyl Derivatives 23 and 27. Amine **4d** (or **4n**) was dissolved in DMA, and the mixture was cooled to 0 °C in an ice bath. Triethylamine (1.1 equiv) and chloroacetyl chloride (0.44 mL, 5.5 mmol) were added. The reaction mixture was stirred at room temperature under nitrogen overnight. Solvent was evaporated under reduced pressure, and to the resulting brown residue was added water and 10% NaHCO₃. Solid was collected by filtration to yield chloride **23** as a white solid (1.03 g, 84%): mp = 287–290 °C; ¹H NMR (DMSO-*d*₆) δ 11.81 (s, 1H), 10.94 (s, 1H), 8.66 (d, 1H), 8.31 (d, 1H), 8.20 (d, 1H), 7.96 (t, 1H), 7.77 (m, 2H), 4.42 (s, 2H). Anal. (C₁₄H₁₀ClN₃O₂) C, H, N.

2-Chloro-N-(6-oxo-5,6-dihydrobenzo[c][1,5]naphthyridin-3-yl)acetamide (27): yield = 87%; mp = 280–284 °C; ¹H NMR (DMSO-*d*₆) δ 11.82 (s, 1H), 10.86 (s, 1H), 8.65 (m, 2H), 8.26 (m, 2H), 7.90 (t, 1H), 7.71 (t, 1H), 4.36 (s, 2H). Anal. (C₁₄H₁₀ClN₃O₂) C, H, N.

General Procedure for the Amination of Chlorides 23 and 27. The chloride **23** (690 mg, 2.4 mmol) was suspended in DMA (20 mL) followed by addition of dimethylamine (2.0 M solution in THF, 6 mL, 12 mmol). The mixture was heated to 80 °C overnight, and the resulting mixture was stripped of solvent and washed with water (50 mL). The resulting solid was suspended in THF followed by addition of HCl (2.0 M in Et₂O, 1.2 mL, 2.4 mmol) and precipitation of a solid. The resulting solid was triturated with diethyl ether and collected via filtration to afford the desired amine **24a** as a white solid (727 mg, 82%).

2-Dimethylamino-N-(6-oxo-5,6-dihydrobenzo[c][1,5]naphthyridin-2-yl)acetamide hydrochloride (24a·HCl):

mp = 195–198 °C; ¹H NMR (D₂O) δ 7.87 (d, 1H), 7.76 (d, 1H), 7.56 (t, 1H), 7.47 (m, 2H), 7.06 (d, 1H), 4.15 (s, 2H), 3.00 (s, 6H). Anal. (C₁₆H₁₆N₄O₂·1.5H₂O·1.0HCl) C, H, N.

N-(6-Oxo-5,6-dihydrobenzo[c][1,5]naphthyridin-2-yl)-2-piperidin-1-ylacetamide hydrochloride (24b·HCl): yield = 87%; mp = 175–180 °C; ¹H NMR (D₂O) δ 8.03 (bd, 1H), 7.90 (d, 1H), 7.66 (t, 1H), 7.59 (d, 1H), 7.54 (t, 1H), 7.22 (d, 1H), 4.12 (s, 2H), 3.63 (s, 2H), 3.13 (s, 2H), 1.86 (m, 6H). Anal. (C₁₉H₂₀N₄O₂·2H₂O·HCl) C, H, N.

N-(6-Oxo-5,6-dihydrobenzo[c][1,5]naphthyridin-2-yl)-2-(4-pyrrolidin-1-ylpiperidin-1-yl)acetamide·HCl (24c·HCl): yield = 92%; mp = 196–200 °C; ¹H NMR (D₂O) δ 7.61 (m, 2H), 7.47 (t, 1H), 7.38 (m, 2H), 6.90 (d, 1H), 3.68 (m, 2H), 3.50 (s, 2H), 3.33 (m, 4H), 2.68 (m, 2H), 2.39 (m, 3H), 1.87–2.12 (m, 6H). Anal. (C₂₃H₂₇N₅O₂·2H₂O·HCl) C, H, N.

2-(4-Isopropylpiperazin-1-yl)-N-(6-oxo-5,6-dihydrobenzo[c][1,5]naphthyridin-2-yl)acetamide hydrochloride (24d·2HCl): yield = 90%; ¹H NMR (D₂O) δ 7.92 (d, 1H), 7.80 (d, 1H), 7.59 (m, 2H), 7.47 (t, 1H), 7.16 (d, 1H), 3.54 (m, 1H), 3.49 (s, 2H), 3.32 (m, 4H), 2.87 (m, 4H), 1.34 (d, 6H). Anal. (C₂₁H₂₅N₅O₂·1.5H₂O·2.0HCl) C, H, N.

2-(3,5-Dinitropyridin-2-yl)-N,N-diisopropylbenzamide (26): yellow foam; yield = 85%; ¹H NMR (CDCl₃) δ 9.55 (d, 1H), 9.05 (d, 1H), 7.51 (m, 2H), 7.39 (t, 2H), 4.02 (bs, 1H), 3.43 (bs, 1H), 1.33 (bs, 6H), 1.20 (bs, 6H). Anal. (C₁₈H₂₀N₄O₅) C, H, N.

3-Amino-5H-benzo[c][1,5]naphthyridin-6-one (4n). The cyclization to form amine **4n** was accomplished through the diamine cyclization with LDA in the same manner as amine **4d** (48%): mp = 300–310 °C; ¹H NMR (DMSO-*d*₆) δ 11.46 (bs, 1H), 8.49 (d, 1H), 8.17 (d, 1H), 7.95 (s, 1H), 7.77 (t, 1H), 7.51 (t, 1H), 6.79 (s, 1H), 5.92 (d, 2H). Anal. (C₁₂H₉N₃O·1.0H₂O) C, H, N.

2-Dimethylamino-N-(6-oxo-5,6-dihydrobenzo[c][1,5]naphthyridin-3-yl)acetamide hydrochloride (28a·HCl): yield = 83%; mp = 285–289 °C; ¹H NMR (D₂O) δ 7.82 (d, 1H), 7.76 (d, 1H), 7.70 (d, 1H), 7.63 (t, 1H), 7.50 (t, 1H), 7.40 (d, 1H), 4.16 (s, 2H), 3.03 (s, 6H). Anal. (C₁₆H₁₆N₄O₂·H₂O·1.0HCl) C, H, N.

N-(6-Oxo-5,6-dihydrobenzo[c][1,5]naphthyridin-3-yl)-2-piperidin-1-ylacetamide hydrochloride (28b·HCl): yield = 82%; ¹H NMR (D₂O) δ 8.03 (bd, 1H), 7.90 (d, 1H), 7.66 (t, 1H), 7.59 (d, 1H), 7.54 (t, 1H), 7.22 (d, 1H), 4.12 (s, 2H), 3.63 (s, 2H), 3.13 (s, 2H), 1.86 (m, 6H). Anal. (C₁₉H₂₀N₄O₂·H₂O·1.0HCl) C, H, N.

N-(6-Oxo-5,6-dihydrobenzo[c][1,5]naphthyridin-3-yl)-2-(4-pyrrolidin-1-ylpiperidin-1-yl)acetamide mesylate (28c·2MsOH): yield = 89%; ¹H NMR (D₂O) δ 7.48 (d, 1H), 7.31 (d, 1H), 7.29 (m, 2H), 7.17 (t, 1H), 6.99 (s, 1H), 3.58 (s, 2H), 3.43–3.31 (m, 5H), 3.22 (m, 2H), 2.91 (m, 2H), 2.74 (m, 2H), 2.48 (s, 6H), 2.14 (m, 2H), 1.89–1.65 (m, 6H). Anal. (C₂₃H₂₇N₅O₂·2H₂O·2MsOH) C, H, N.

2-(4-Dimethylaminopiperidin-1-yl)-N-(6-oxo-5,6-dihydrobenzo[c][1,5]naphthyridin-3-yl)acetamide hydrochloride (28d·HCl): yield = 89%; ¹H NMR (D₂O) δ 7.78 (d, 1H), 7.60 (m, 3H), 7.50 (t, 1H), 7.23 (s, 1H), 3.74 (m, 3H), 3.47 (s, 2H), 3.40 (m, 4H), 2.90 (m, 2H), 1.55 (d, 6H). Anal. (C₂₁H₂₅N₅O₂·2.25H₂O·1HCl) C, H, N.

PARP-1 Inhibition Assay. Purified recombinant human PARP from Trevigan (Gaithersburg, MD) was used to determine the IC₅₀ values of a PARP inhibitor. The PARP enzyme assay is set up on ice in a volume of 100 μL consisting of 50 mM Tris-HCl (pH 8.0), 2 mM MgCl₂, 30 μg/mL of DNase activated herring sperm DNA (Sigma, MO), 30 μM [³H]-nicotinamide adenine dinucleotide (67 mCi/mmol), 75 μg/mL PARP enzyme, and various concentrations of the compounds to be tested. The reaction is initiated by incubating the mixture at 25 °C. After 15 min of incubation, the reaction was terminated by adding 500 μL of ice-cold 20% (w/v) trichloroacetic acid. The precipitate formed is transferred onto a glass fiber filter (Packard Unifilter-GF/B) and washed three times with ethanol. After the filter is dried, the radioactivity is determined by scintillation counting.

Methods for Determining EC₅₀ Values. The H₂O₂ cytotoxicity assay was utilized for EC₅₀ determination as outlined by our group in a previous publication.²⁵ P388D1 cells (CCL-46, ATCC, Rockville, MD), derived from murine-macrophage-like tumor, were maintained in Dulbecco's modified Eagle medium (DMEM) with 10% horse serum and 2 mM L-glutamine. The cytotoxicity assay was set up in a 96-well plate. In each well, 190 μL cells were seeded at 2 × 10⁶/mL density. To determine the EC₅₀, the concentration of a compound required to achieve 50% reduction of cell death, a dose-responsive experiment was conducted. The inhibitors were added to the media with final concentrations of 0.01, 0.03, 0.1, 0.3, 1, 3, 10, and 30 μM. Each data point was an average of quadruplicate measurements. After 15 min of incubation with the inhibitors, 5 μL of freshly prepared H₂O₂ was added to the cells to a final concentration of 2 mM. Cells were returned to a 37 °C incubator for 4 h. At the end of the incubation, 25 μL of supernatant were sampled from the cell media to determine the level of lactate dehydrogenase released from dead cells. We used an LDH assay adapted from Sigma Co. (St. Louis, MO) and followed the experimental procedure according to the manufacturer. The LDH activity was determined by monitoring the rate of decrease of NADH absorbency at 340 nm. Background LDH activity was subtracted. The group without drug treatment was used to calculate total cell death due to H₂O₂ treatment. The EC₅₀ was determined from a dose-response curve.

Methods for Solubility Testing. The solubility data was recorded by a Nepheloskan Ascent Instrument, type 750 manufactured by Labsystems. The instrument settings were the following: PMT voltage = 300; lamp voltage = 10.0. The first step is to prepare the vehicles in which solubility values are desired. The following vehicles were used for evaluation: 50 mM citrate buffer (pH 4.0), 70 mM phosphate buffer saline (PBS) (pH 7.4). Citrate buffer was prepared by dissolving 10.5 g of citric acid in 1000 mL of deionized (DI) water and adjusting the pH using 10 N NaOH. PBS was prepared by dissolving 1.9 g of KH₂PO₄, 8.1 g of Na₂HPO₄, and 4.1 g of NaCl in 1000 mL of DI water and adjusting the pH using 10 N NaOH. The test compounds were dissolved in the vehicle at 5 mg/mL. The mixtures were vortexed for 5 s, sonicated for 10 min at 37 °C, and then vortexed again for 5 s. The samples (400 μL of each) were transferred to a 96-well plate and immediately analyzed for turbidity.

Methods for Evaluating the Degradation of 4g in Microsomal Enzymes. Compound **4g**·MsOH (100 μM) was incubated with pooled liver microsomes (0.1 or 1.0 mg/mL) from rat, dog, monkey, or human and with an NADPH-generating system (1 mM NADP⁺, 10 mM glucose 6-phosphate, 1 U/mL glucose 6-phosphate dehydrogenase, 5 mM MgCl₂) in 100 mM potassium phosphate buffer, pH 7.4. The reactions were initiated by substrate addition. Incubations were carried out at 37 °C. Aliquots of 300 μL were withdrawn at various time points and mixed with 500 μL of acetonitrile to stop the reaction. Quantitation was performed on an LC/MS/MS system consisting of an Agilent 1100 HPLC system with a YMC basic reversed-phase column coupled to a Micromass Ultima mass spectrometer.

Methods for Evaluating Pharmacokinetic Samples of 4g, 4l, 4j, 4m, and 24c. The selected PARP-1 inhibitors were dosed as an intravenous bolus into male Wistar rats at 10 mg/kg over 5 min (5 mL total volume). One animal was sacrificed at each time point, and samples from the desired tissues or plasma were collected and assayed as described below.

Sample Preparation. The calibration standards covered the range 1–1000 ng/mL. The quality control (QC) standard ranges were 3, 30, 300, and 800 ng/mL. A 1:10 dilution of the 800 ng/mL QC sample was run. Sample from tissue, calibration standards, and QC samples were subjected to protein precipitation by acetonitrile followed by filtration in an Anasys, Captiva 96-well filter plate. All samples were analyzed on a LC/MS/MS (MicroMass Ultima) with an electrospray source in positive ion mode.

Analytical Method for 4g. Mobile phase: isocratic, acetonitrile (ACN), and 0.1% formic acid in water. Column: YMC Basic, 3 μm , 4.0 mm \times 50.0 mm. Injection volume: 10 μL .

Analytical Method for 4j. Mobile phase: gradient of ACN and 10 mM NH_4AC (ammonium acetate), 15–75% ACN linear gradient from 0 to 2.0 min was run, followed by isocratic 75% ACN until 2.4 min. From 2.4 to 4.0 min, the column was reequilibrated at 15% ACN. Column: Phenomenex Aqua, 3 μm C18 125A, 30 mm \times 4.60 mm. Injection volume: 10 μL .

Analytical Method for 4m. Mobile phase: gradient of ACN and 10 mM NH_4AC (ammonium acetate), 15–75% ACN linear gradient from 0 to 2.0 min was run, followed by isocratic 75% ACN until 2.4 min. From 2.4 to 4.0 min, the column was reequilibrated at 15% ACN. Column: Phenomenex Aqua, 3 μm C18 125A, 30 mm \times 4.60 mm. Injection volume: 20 μL .

Analytical Method for 4l. Mobile phase: gradient of ACN and 10 mM NH_4AC (ammonium acetate), 15–75% ACN linear gradient from 0 to 2.0 min was run, followed by isocratic 75% ACN until 2.4 min. From 2.4 to 4.0 min, the column was reequilibrated at 15% ACN. Column: YMC Basic, 3 μm , 4.0 mm \times 50.0 mm. Injection volume: 10 μL .

Analytical Method for 24c. Mobile phase: isocratic, acetonitrile (ACN), and 0.1% formic acid in water. Column: YMC Cyno, 3 μm 120A, 30 mm \times 50.0 mm. Injection volume: 25 μL .

Method for Testing PARP Inhibitors in Focal Cerebral Ischemic Stroke. Transient focal ischemic stroke was modeled in rats using the intraluminal thread procedure as modified by Belayev.³¹ Male Sprague–Dawley rats (280–320 g, Charles River, Wilmington, MA) were anesthetized with isoflurane. A polylysinized 3–0 suture was inserted through the internal carotid artery into the origin of the middle cerebral artery (MCA). The suture is removed after 2 h of MCA occlusion.

Permanent focal cerebral ischemic stroke was modeled in rats using a modification of the method described by Chen et al.³² Male Long Evans rats (280–350 g, Harlan-Sprague Dawley, Indianapolis, IN) were anesthetized with isoflurane. The right and left common carotid arteries and the right distal MCA were exposed and isolated. The distal MCA was cauterized, and the carotids were transiently occluded for 90 min.³⁶

All drugs were administered 30 min after the start of MCA occlusion. For both models, the brains were collected into cold PBS at 24 h after ischemia. The brains were sliced and processed for TTC histochemistry, and the apparent infarcts were measured using computer-assisted planimetry. In the transient paradigm, total infarcts average 350 mm³ including both cortical and subcortical tissue. In the permanent model, the infarcts were exclusively cortical and averaged 180 mm³. The effect of drug treatment is expressed as the percent reduction in infarct volume compared to coincident vehicle controls. Statistical significance was determined using the Student *t* test with a confidence interval accepted when $p \leq 0.05$.

Method for Testing PARP Inhibitors in Myocardial Ischemia Assay.³³ The compounds were solubilized in either 70 mM phosphate-buffered saline (4g) or 50 mM citrate buffer (4m and 24c). The only deviation from the literature assay was that half of the desired compound was administered as a bolus dose 5 min before the ischemic event and the other half of the compound was given as a bolus dose 5 min before reperfusion.

References

- Herceg, Z.; Wang, Z. Q. Failure of poly(ADP-ribose) polymerase cleavage by caspases leads to induction of necrosis and enhanced apoptosis. *Mol. Cell. Biol.* **1999**, *19*, 5124–5133.
- Decker, P.; Isenberg, D.; Muller, S. Inhibition of caspase-3-mediated poly(ADP-ribose) polymerase (PARP) apoptotic cleavage by human PARP autoantibodies and effect on cells undergoing apoptosis. *J. Biol. Chem.* **2000**, *275*, 9043–9046.
- Yu, S.-W.; Wang, H.; Poitras, M. F.; Coombs, C.; Bowers, W. J.; Federoff, H. J.; Poirer, G. G.; Dawson, T. M.; Dawson, V. L. Mediation of Poly(ADP-ribose) Polymerase-1-Dependent Cell Death by Apoptosis-Inducing Factor. *Science* **2002**, *297*, 259–263.
- Rolli, V.; O'Farrell, M.; Menissier-de Murcia, J.; de Murcia, G. Random mutagenesis of the poly(ADP-ribose) polymerase catalytic domain reveals amino acids involved in polymer branching. *Biochemistry* **1997**, *36*, 12147–12154.
- de Murcia, G.; Schreiber, V.; Molinete, M.; Saulier, B.; Poch, O.; Masson, M.; Niedergang, C.; Menissier de Murcia, J. Structure and function of poly(ADP-ribose) polymerase. *Mol. Cell. Biochem.* **1994**, *138*, 15–24.
- Jeggo, P. A. DNA repair: PARP—another guardian angel? *Curr. Biol.* **1998**, *8*, R49–R51.
- Takahashi, K.; Pieper, A. A.; Croul, S. E.; Zhang, J.; Snyder, S. H.; Greenberg, J. H. Post-treatment with an inhibitor of poly(ADP-ribose) polymerase attenuates cerebral damage in focal ischemia. *Brain Res.* **1999**, *829*, 46–54.
- Nagayama, T.; Simon, R. P.; Chen, D.; Henshall, D. C.; Pei, W.; Stetler, R. A.; Chen, J. Activation of poly(ADP-ribose) polymerase in the rat hippocampus may contribute to cellular recovery following sublethal transient global ischemia. *J. Neurochem.* **2000**, *74*, 1636–1645.
- Eliasson, M. J.; Sampei, K.; Mandir, A. S.; Hurn, P. D.; Traystman, R. J.; Bao, J.; Pieper, A.; Wang, Z. Q.; Dawson, T. M.; Snyder, S. H.; Dawson, V. L. Poly(ADP-ribose) polymerase gene disruption renders mice resistant to cerebral ischemia. *Nat. Med.* **1997**, *3*, 1089–1095.
- Pieper, A. A.; Wallis, T.; Wei, G.; Clements, E. E.; Verma, A.; Snyder, S. H.; Zweier, J. L. Myocardial postischemic injury is reduced by polyADP-ribose polymerase-1 gene disruption. *Mol. Med.* **2000**, *6*, 271–282.
- Abdelkarim, G. E.; Gertz, K.; Harms, C.; Katchanov, J.; Dirnagl, U.; Szabo, C.; Endres, M. Protective effects of PJ34, a novel, potent inhibitor of poly(ADP-ribose) polymerase (PARP) in vitro and in vivo models of stroke. *Int. J. Mol. Med.* **2001**, *7*, 255–260.
- Watson, C. Y.; Whish, W. J.; Threadgill, M. D. Synthesis of 3-substituted benzamides and 5-substituted isoquinolin-1(2*H*)-ones and preliminary evaluation as inhibitors of poly(ADP-ribose)polymerase (PARP). *Bioorg. Med. Chem.* **1998**, *6*, 721–734.
- Griffin, R. J.; Srinivasan, S.; Bowman, K.; Calvert, A. H.; Curtin, N. J.; Newell, D. R.; Pemberton, L. C.; Golding, B. T. Resistance-modifying agents. 5. Synthesis and biological properties of quinazolinone inhibitors of the DNA repair enzyme poly(ADP-ribose) polymerase (PARP). *J. Med. Chem.* **1998**, *41*, 5247–5256.
- Li, J. H.; Serdyuk, L.; Ferraris, D. V.; Xiao, G.; Tays, K.; Kletzly, P. W.; Li, W.; Lautar, S.; Zhang, J.; Kalish, V. Synthesis of 5[*H*]-Phenanthridin-6-ones as potent poly(ADP-ribose)polymerase-1 (PARP1) inhibitors. *Bioorg. Med. Chem. Lett.* **2001**, *11*, 1687–1690.
- Ruf, A.; de Murcia, G.; Schulz, G. E. Inhibitor and NAD⁺ binding to poly(ADP-ribose) polymerase as derived from crystal structures and homology modeling. *Biochemistry* **1998**, *37*, 3893–3900.
- White, A. W.; Almassy, R.; Calvert, A. H.; Curtin, N. J.; Griffin, R. J.; Hostomsky, Z.; Maegley, K.; Newell, D. R.; Srinivasan, S.; Golding, B. T. Resistance-modifying agents. 9. Synthesis and biological properties of benzimidazole inhibitors of the DNA repair enzyme poly(ADP-ribose) polymerase. *J. Med. Chem.* **2000**, *43*, 4084–4097.
- Canan Koch, S. S.; Thoresen, L. H.; Jayashree, G. T.; Maegley, K. A.; Almassy, R. J.; Li, J.; Yu, X.-H.; Zook, S. E.; Kumpf, R. A.; Zhang, C.; Boritzki, T. J.; Mansour, R. N.; Zhang, K. E.; Ekker, A.; Calabrese, C. R.; Curtin, N. J.; Kyle, S.; Thomas, H. D.; Wang, L.-Z.; Calvert, A. H.; Golding, B. T.; Griffin, R. J.; Newell, D. R.; Webber, S. E.; Homstomsky, Z. Novel tricyclic poly(ADP-ribose) polymerase-1 inhibitors with potent anticancer chemopotentiating activity: Design, synthesis and X-ray cocrystal structure. *J. Med. Chem.* **2002**, *45*, 4961–4974.
- Shinkwin, A. E.; Whish, W. J.; Threadgill, M. D. Synthesis of thiophenecarboxamides, thieno[3,4-*c*]pyridin-4(5*H*)-ones and thieno[3,4-*d*]pyrimidin-4(3*H*)-ones and preliminary evaluation as inhibitors of poly(ADP-ribose)polymerase (PARP). *Bioorg. Med. Chem.* **1999**, *7*, 297–308.
- Rocca, P.; Cochenec, C.; Marsais, F.; Thomas-dit-Dumont, L.; Mallet, M.; Godard, A.; Queguiner, G. First Metalation of Aryl Iodides: Directed Ortho-Lithiation of Iodopyridines, Halogen-Dance, and Application to Synthesis. *J. Org. Chem.* **1993**, *58*, 7832–7838.
- Park, Y.-T.; Jung, C.-H.; Kim, M.-S.; Kim, K.-W. Photoreaction of 2-Halo-*N*-pyridinylbenzamide: Intramolecular Cyclization Mechanism of Phenyl Radical Assisted with *n*-Complexation of Chlorine Radical. *J. Org. Chem.* **2001**, *66*, 2197–2206.
- Rocca, P.; Marsais, F.; Godard, A.; Queguiner, G. Connection between Metalation and Cross-Coupling Strategies. A New

- Convergent Route to Azacarbazoles. *Tetrahedron* **1993**, *49*, 49–64.
- (22) Guillier, F.; Nivoliers, F.; Godard, A.; Marsais, F.; Queguiner, G.; Siddiqui, M. A.; Snieckus, V. Combined Metalation–Palladium-Catalyzed Cross Coupling Strategies. A Formal Synthesis of the Marine Alkaloid Amphimedine. *J. Org. Chem.* **1995**, *60*, 292–296.
- (23) Kristensen, J.; Lysen, M.; Vedso, P.; Begtrup, M. Synthesis of ortho substituted arylboronic esters by in situ trapping of unstable lithio intermediates. *Org. Lett.* **2001**, *3*, 1435–1437.
- (24) Banasik, M.; Komura, H.; Shimoyama, M.; Ueda, K. Specific inhibitors of poly(ADP-ribose)synthetase and mono(ADP-ribose)transferase. *J. Biol. Chem.* **1992**, *267*, 1569–1575.
- (25) Zhang, J.; Lautar, S.; Huang, S.; Ramsey, C.; Cheung, A.; Li, J. H. GPI 6150 prevents H₂O₂ cytotoxicity by inhibiting poly(ADP-ribose) polymerase. *Biochem. Biophys. Res. Commun.* **2000**, *278*, 590–598.
- (26) Beyan, C. D.; Lloyd, R. S. A high throughput screening method for the determination of aqueous drug solubility using laser nephelometry in microtiter plates. *Anal. Chem.* **2000**, *72*, 1781–1787.
- (27) The structure of compound **41** was deduced from ¹H NMR.
- (28) Bergstad, K.; Backvall, J. E. Mild and Efficient Flavin-Catalyzed H₂O₂ Oxidation of Tertiary Amines to Amine N-Oxides. *J. Org. Chem.* **1998**, *63*, 6650–6655.
- (29) Guengerich, F. P. Cytochrome P450. *Enzyme Systems That Metabolise Drugs and Other Xenobiotics*; Wiley-VCH: Weinheim, Germany, 2002; pp 33–67.
- (30) Silverman, R. B. Pathways for Drug Deactivation and Elimination. *The Organic Chemistry of Drug Design and Drug Action*; Academic Press: London, 1992; pp 287–351.
- (31) Belayev, L. Middle cerebral artery occlusion in the rat by intraluminal suture. Neurological and pathological evaluation of an improved model. *Stroke* **1996**, *27*, 1616–1622.
- (32) Chen, S. T. A model of focal ischemic stroke in the rat: reproducible extensive cortical infarction. *Stroke* **1986**, *17*, 738–743.
- (33) Wayman, N.; McDonald, M. C.; Thompson, A. S.; Threadgill, M. D.; Thiemeermann, C. 5-Aminoisoquinoline, a potent inhibitor of poly(adenosine 5'-phosphate ribose) polymerase, reduces myocardial infarct size. *Eur. J. Pharmacol.* **2001**, *430*, 93–100.
- (34) Kukreja, R. C.; Qian, Y. Z.; Okubo, S.; Flaherty, E. E. Role of protein kinase C and 72 kDa heat shock protein in ischemic tolerance following heat stress in the rat heart model. *Mol. Cell. Biochem.* **1999**, *195*, 123–131.
- (35) Romanelli, M. N.; Manetti, D.; Scapecchi, S.; Borea, P. A.; Dei, S.; Bartolini, A.; Ghelardini, C.; Gualtieri, F.; Guandalini, L.; Varani, K. Structure–activity relationships of a unique nicotinic ligand: N1-Dimethyl-N4-phenylpiperazinium iodide (DMPP). *J. Med. Chem.* **2001**, *44*, 3946–3955.
- (36) Takahashi, K.; Greenberg, J. H.; Jackson, P.; Maclin, K.; Zhang, J. Neuroprotective effects of inhibiting poly(ADP-ribose) synthetase on focal cerebral ischemia in rats. *J. Cereb. Blood Flow Metab.* **1997**, *17*, 1137–1142.

JM030109S